POLITECNICO
MILANO 1863

INSTITUTO DE
TECNOLOGÍA
QUÍMICA

School of Industrial and Information Engineering
Master of Science in Chemical Engineering

Computational modeling and economical assessment of an Oxygen Transport Membrane (OTM) oxy-combustion reactor for heat recovery from a pyrolysis unit

Candidate
Federica Roccaro
Code 921239

Thesis Supervisor
Prof. Filippo Rossi

Tutors
David Catalán Martínez
Julio García Fayos

Academic Year 2019 / 2020

A Gaia, mamma, papà e Daniele

Contents

List of figures

List of tables

List of equations

Abstract

Plastic materials disposal has become a topic of outmost importance in the last few years. We are witnessing an increasing production of plastics and dependance on its usage, while the recycling techniques are almost unchanged throughout the years, with a very low recycling efficiency: around 70% of wasted plastic is being burnt or sent to landfill.

iCAREPLAST is a project funded by the European Union to implement a chemical recycling route of plastics: useful chemicals can be produced, at a very high efficiency rate, in an outlook of circular economy. Such process comprehends a preliminary pyrolysis process of all treated plastics put together, and subsequent catalytic reaction steps to obtain the desired final products.

In the pyrolysis section, also gaseous hydrocarbons are produced, which are useless for the purpose. To enhance the energetic efficiency of the process, these gases can undergo a controlled, oxy-combustion reaction, to produce a great quantity of heat to be recycled in the plant. An Oxygen Transport Membrane (OTM) reactor would help to reach high control of the reactor, high efficiency, and low volumes. Due to its nature, it is a non-conventional unit that requires a proper design process. The aim of this study is to put the basis for the design, decision-making process linked to the oxy-combustion section of such recycle plant.

Starting from the modeling of the reacting unit, it was possible to obtain feasible, numerical results as an outlet of a computational model. Then, a proper reactor configuration was hypothesized, and a qualitative, parametric study on the reactor allowed a better comprehension of the internal dynamic of the process and of the variables to be accounted for in the design process. Eventually, a plant design hypothesis brought to the formulation of the variation of the economic potential in function of such variables, a tool that can be useful in the decision-making process.

Sintesi

Lo smaltimento di materiale plastico è diventato un argomento di grande importanza negli ultimi anni. Assistiamo ad una crescita nella produzione di plastica, e al contempo ad una sempre crescente dipendenza dal suo utilizzo, mentre le tecniche di riciclo rimangono quasi immutate negli anni, con un'efficienza di riciclo molto bassa: circa il 70% dei rifiuti plastici viene bruciato o mandato a discarica.

Il progetto iCAREPLAST, in collaborazione con l'Unione Europea, punta a implementare un processo di riciclo chimico delle plastiche: monomeri utili vengono prodotti, con un'efficienza di riciclo molto elevata, in un'ottica di economia circolare. Tale processo prevede uno step preliminare di pirolisi di tutte le plastiche trattate complessivamente e reazioni catalitiche successive per ottenere finalmente i prodotti desiderati.

Nella sezione di pirolisi vengono prodotti anche idrocarburi gassosi non utili per il processo. Per migliorare l'efficienza energetica del processo, questi gas possono subire un trattamento controllato di ossicombustione, in modo da produrre una grande quantità di calore che può essere riciclato nell'impianto. Un reattore costituito da sistemi di *Oxygen Transport Membrane* (OTM) risulta funzionale allo scopo, garantendo alti livelli di controllo, alte efficienze e volumi contenuti. Data la sua natura, va disegnata opportunamente come unità non convenzionale. L'obiettivo di questo studio è mettere le basi per il processo di *design* e per prendere decisioni economiche per la sezione di ossicombustione di questo impianto di riciclo.

Partendo dalla modellazione del reattore, è stato possibile ottenere risultati numerici veritieri come *outlet* di un modello informatico. In seguito, è stata ipotizzata un'opportuna configurazione reattoristica, e uno studio parametrico qualitativo ha permesso una migliore comprensione delle dinamiche interne del processo e delle variabili da considerare nel processo di *design*. Infine, un'ipotesi di *design* dell'impianto ha portato alla formulazione della variazione del potenziale economico in funzione di tali variabili, uno strumento che può essere utile per prendere decisioni economiche.

1. Introduction

1.1 Plastic demand: an increasing issue

Plastic materials disposal has become a topic of utmost importance in the last few years. This issue is related to the yearly increasing production of plastics worldwide (Figure 1). In 2018 only, 359 million tons of plastics were produced worldwide, of which 61.8 Mt in Europe: plastics are extensively used in the sectors of packaging, consumer and household goods, and constructions [1].

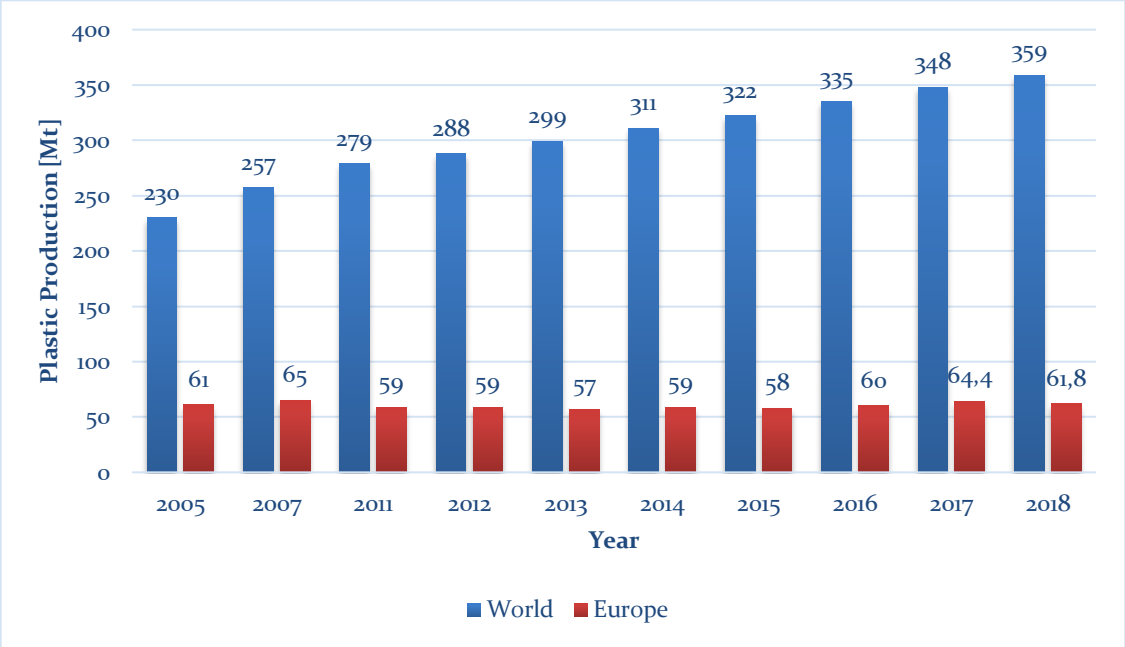

Figure 1: Yearly Plastics Production [2, 3, 4, 5]

In Europe in 2018, 29.1 Mt of plastic were collected to be disposed of, of which 17.8 Mt (62% of the total) were coming from packaging waste [1] – everyday life waste. A huge problem of environmental pollution arises from its incorrect disposal: of all the plastic waste in a year in Europe, only 32.5% was recycled in 2018 [6].

Since 2006, the total quantity of plastic waste sent to recycling facilities increased twofold (Figure 2). Nevertheless, although landfilled quantities decreased by 44% compared to 2006, with an average annual fall rate of 4.7%, 7.2 Mt of plastic waste still ended up in landfill in 2018 [6].

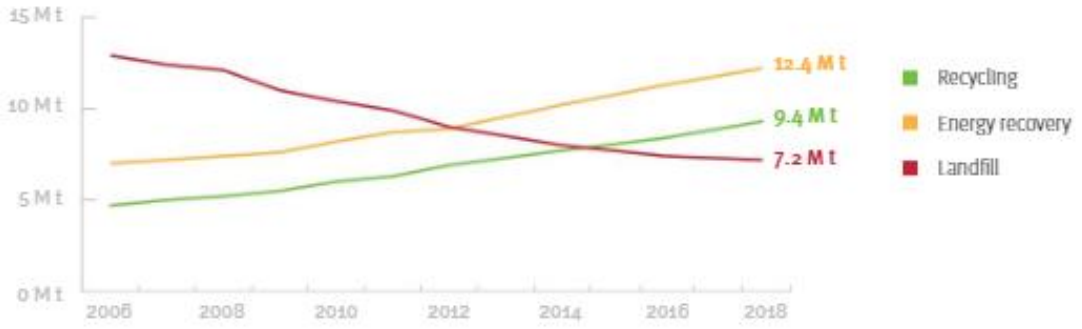

Figure 2: Waste treatment options for post-consumer plastic waste 2006-2018 in EU28+2 [6]

When it comes to packaging waste, the situation changes (Figure 3). The quantity of packaging plastic waste sent to landfill decreased by 54% compared to 2006 and recycled plastic increased by more than 92% [6]. This shows that in the European Union the importance of a correct waste treatment, like for instance a correct sorting practice, has been emphasized, and eventually the capacity of the recycle facilities was enhanced.

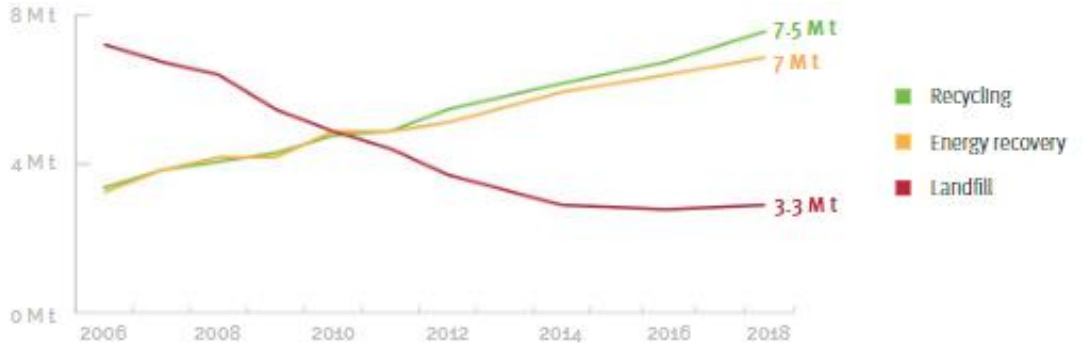

Figure 3: Waste treatment options for post-consumer plastic packaging waste 2006-2018 in EU28+2

1.2 Plastic recycling state of the art

Plastic recycling techniques improved increasingly due to the exponentially increasing amount of plastic to be treated worldwide. These can be divided in four types mainly (Figure 4) [7]:

- **Primary** recycle, which consists of simple cleaning procedures to use a piece of plastic with the same features of the end use polymer [7].

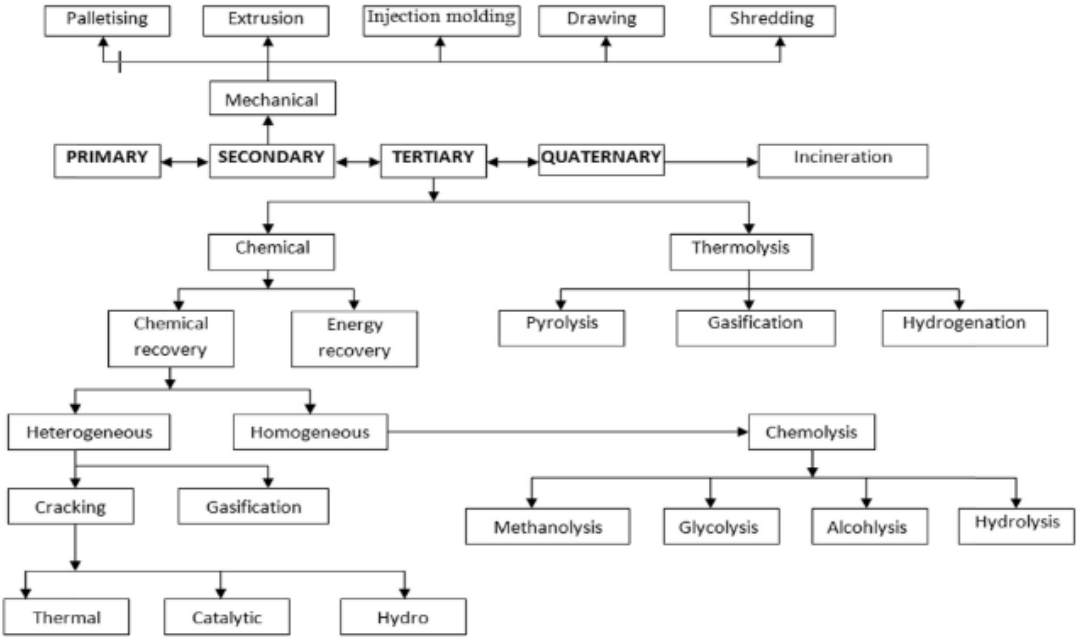

Figure 4: Various approaches for recycling plastic solid waste [7]

- **Secondary** recycle, also called **mechanical** recycle. The preliminary operations preceding this process are schematized below (Figure 5):

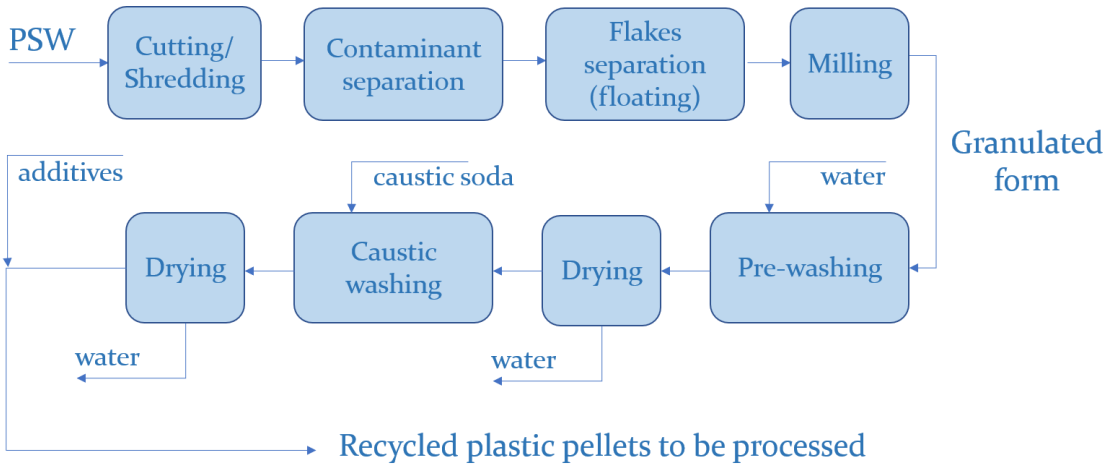

Figure 5: Preliminary operations to secondary recycle [7]

It can be carried via palletizing, extrusion (the most common in polymeric film production), injection molding, drawing, and shredding.

- **Tertiary recycle** involving chemical reactions, in particular catalytic paths, energy recovery processes and thermolysis.
- **Quaternary recycle** or simple incineration.

The main recycle route currently used in Europe is mechanical recycle, with just 0.1 Mt undergoing chemical recycling. Of course, mechanical recycle has some efficiency, as for instance the recycling rate for packaging plastics lowers from 42% to 29% when the preliminary procedures are applied (Figure 6). This means that the remainder is sent to landfill (27%) or incinerated for energy recovery (42%).

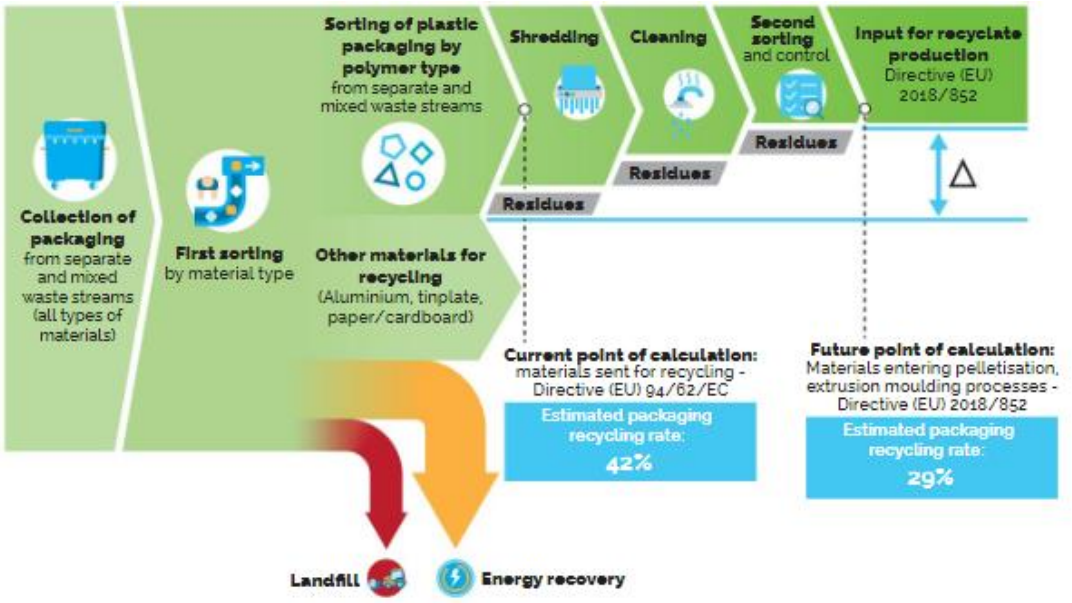

Figure 6: Estimated packaging recycling rate change due to preliminary operations [6]

A large part of the efficiency of the process is being detracted by the *sorting* procedure: plastic waste must be sorted by polymer type and these are to be treated separately. This affects the overall process by making *multilayer plastic packaging*, constituted by layers made of different polymers, *unrecyclable*.

1.3 iCAREPLAST: a game-changing technology

In the European plastic-disposal scenario, a project took life from the cooperation of the Consejo Superior de Investigaciones Científicas (CSIC) and several partners from all over the European Community, including companies and universities. Its

name is iCAREPLAST, acronym for *Integrated Catalytic Recycling of Plastic Residues into Added-Value Chemicals* [8].

Figure 7: iCAREPLAST logo [8].

The purpose of the project is demonstrating a whole new plastic waste valorization technology in a pilot plant able to process more than 80 kg/h of plastic. The plastic to be treated will undergo a *tertiary recycle* process, comprising a thermolysis (pyrolysis) section and some catalytic reactions that will lead to the production of alkylbenzenes and BTX – very valuable chemicals [8].

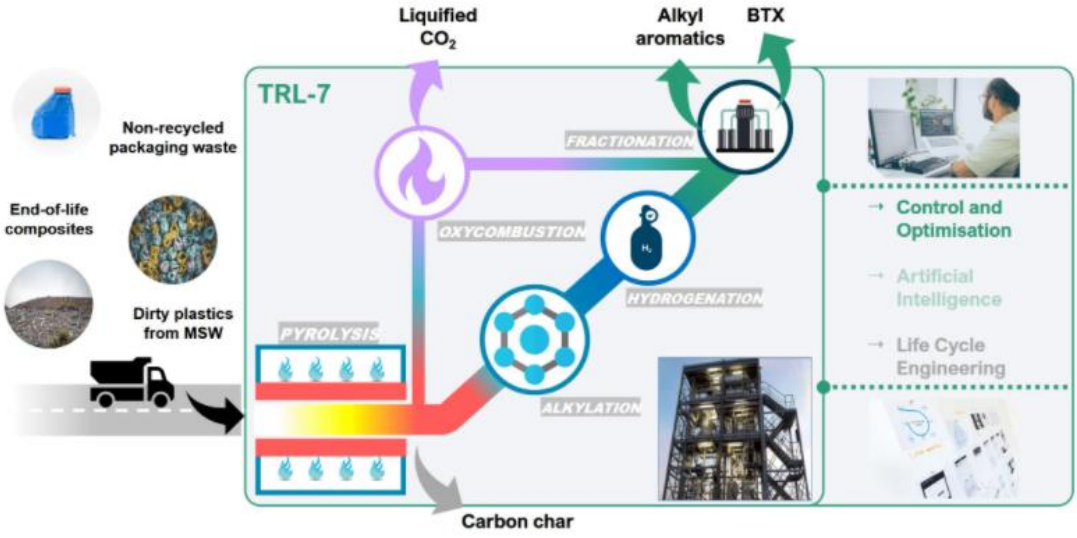

Figure 8: Overall Concept behind iCAREPLAST Process [8]

The main sections of the plant are (Figure 8):

- The *pyrolysis* section, in which plastics are burnt and melted to be converted to smaller, useful molecules. Besides, a gas current and a carbon char current leave the section.
- The *alkylation* section and the *hydrogenation* one, which consist of sequential catalytic steps.

- The *fractionation* section, from which it is possible to obtain the products of interest and a lighter gas current.
- The *oxy-combustion* section, where gases leaving the pyrolysis section and the fractionation section are converted to a more valuable CO_2 current.

The main advantages of such recycling route are:

- **Any plastic waste** can undergo pyrolysis: this means that the amount of recyclable plastics could increase, avoiding landfill waste amassing and waste incineration. As a proof of this, the purpose of the iCAREPLAST project is to treat 250,000 t of plastic waste which otherwise, due to the currently available technologies, would become landfill [8].
- The products obtained from the process can be used for many purposes, in the petrochemical and fine chemical industries (such as detergent and surfactant industries), and also for polymers production, to enhance plastics **circular economy** (Figure 9).

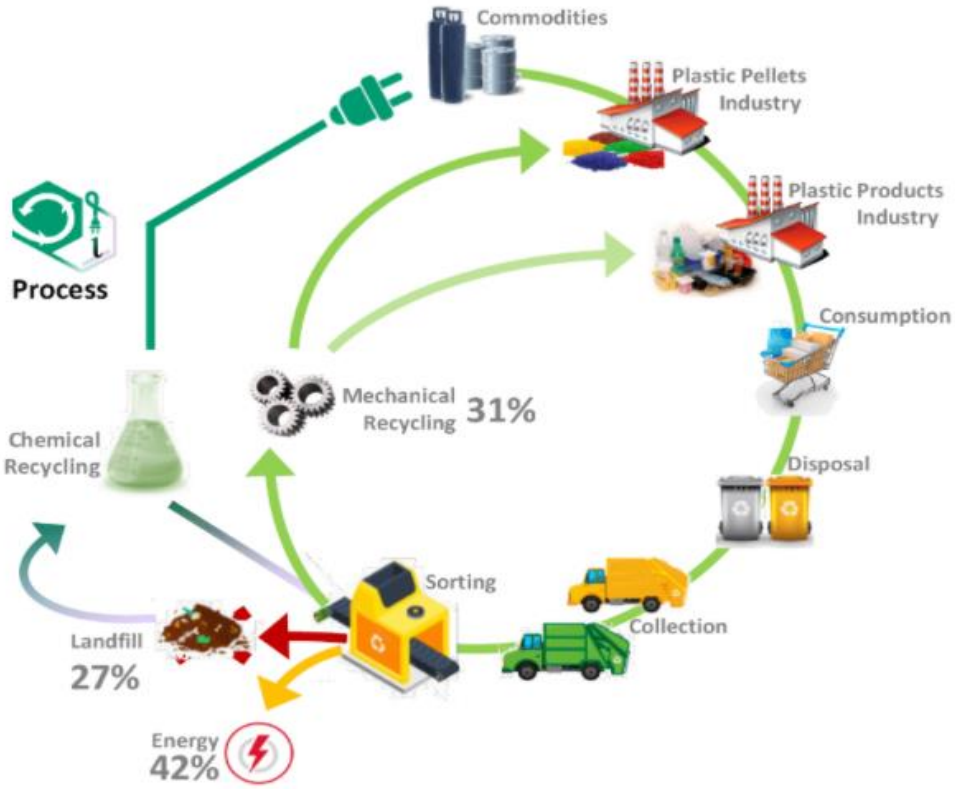

Figure 9: Plastics circular economy enhancement using the iCAREPLAST solution [8].

- The polymers produced starting from the obtained products will be **virgin-quality polymers**, unlike currently recycled plastics – for instance, in Europe the use of functional barriers in multilayer polymers in contact with food is mandatory when a recycled polymer is used, to meet the requirements stated by the European Commission in terms of food contamination [9].
- **Subproducts** of the process like CO_2 and char are recovered and **valorized** to maximize the yield of the process, reduce the environmental footprint, and ensure economic sustainability [8].

1.4 Gas recovery and the oxy-combustion section

In the frame of iCAREPLAST project, a series of tests was executed in the pyrolysis pilot section in order to characterize the resulting pyrolytic streams. The weight yield of liquid, gas, and solid products per kg of plastic was obtained from theoretical models [10] [11] [12] [13] [14] [15] [16] [17] [18] [19] [20] [21] [22] [23] [24] [25] [26] [27] [28] [29] [30] [31] [32] [33] [34] [35] and adapted to experimental results, at different pyrolysis temperatures for each kind of plastic treated: polyethylene (Table 1: Weight yields for polyethylene pyrolysis [kg/kg of plastics]), polypropylene (Table 2), and polystyrene (Table 3).

The liquid stream is the one of main interests for the iCAREPLAST process, while the solid stream is substantially a carbon char stream and the gaseous stream contains light hydrocarbons. Also, the gaseous stream composition was analyzed for each current (Table 4: Molar composition of the gas stream leaving the pyrolysis section for polyethylene[%], Table 5, Table 6).

Hydrocarbons leaving the pyrolysis section in the gaseous stream range from 1 to 6 carbon atoms, and (usually) the fraction of lighter hydrocarbons increases with the pyrolysis temperature, which is between 400 and 500 °C. It also contains a small fraction of hydrogen.

This gas fraction is useless for the subsequent process, whose aim is to produce alkylbenzenes and BTX which have at least 6 carbon atoms: Therefore, this fraction has been valorized in the process to obtain heat in an *oxy-combustion* process, a

combustion carried in presence of oxygen only, instead of air. The oxy-combustion approach also allows to separate the CO_2 generated in the combustion reactions.

Table 1: Weight yields for polyethylene pyrolysis [kg/kg of plastics]

T (°C)	400	410	420	430	440	450	460	470	480	490	500
Liquid	82.39	84.23	85.65	86.64	87.24	87.41	87.17	86.50	85.42	83.93	82.02
Gas	**16.69**	**14.63**	**12.99**	**11.80**	**10.96**	**10.57**	**10.59**	**11.04**	**11.90**	**13.17**	**14.87**
Solid	0.92	1.14	1.36	1.56	1.80	2.02	2.24	2.46	2.68	2.90	3.12

Table 2: Weight yields for polypropylene pyrolysis [kg/kg of plastics]

T (°C)	300	325	350	375	400	425	450	475	500	525	550	575	600	625	650	675	700
Liquid	52.00	61.56	69.75	76.56	82.00	86.06	88.75	90.06	90.00	88.56	85.75	81.56	76.00	69.06	60.75	51.06	40.00
Gas	**14.17**	**13.35**	**11.65**	**9.64**	**7.77**	**6.35**	**5.63**	**5.77**	**6.91**	**9.14**	**12.55**	**17.18**	**23.07**	**30.24**	**38.74**	**48.56**	**59.72**
Solid	33.83	25.09	18.60	13.79	10.23	7.58	5.62	4.17	3.09	2.29	1.70	1.26	0.93	0.69	0.51	0.38	0.28

Table 3: Weight yields for polystyrene pyrolysis [kg/kg of plastics]

T (°C)	350	375	400	425	450	475	500	525	550
Gas	**3.0622**	**7.3886**	**6.3953**	**5.0478**	**5.7613**	**9.7621**	**17.6979**	**29.9221**	**46.6338**
Liquid	47.6550	64.9863	77.5300	85.2863	88.2550	86.4363	79.8300	68.4363	52.2550
Solid	49.2828	27.6251	16.0747	9.6659	5.9838	3.8016	2.4721	1.6417	1.1112

Table 4: Molar composition of the gas stream leaving the pyrolysis section for polyethylene[%]

T	H2	CH4	C2H4	C2H6	C3H6	C3H8	C4H10(ISO)	C4H8	C4H10(N)	C4H8	C4H6	C5H10	C6H12
400	4.0098	16.4499	6.5985	15.3848	10.0217	10.6061	0.3515	4.1668	4.4155	24.8553	1.2946	1.1602	0.6853
410	4.7987	15.6665	6.2843	14.6522	9.5445	10.1010	0.3700	4.3862	4.6479	26.1635	1.3628	1.2611	0.7614
420	5.3392	14.9205	5.9850	13.9545	9.0900	9.6200	0.3895	4.6170	4.8925	27.5405	1.4345	1.3708	0.8460
430	4.7400	14.2100	5.7000	13.2900	9.0900	9.6200	0.4100	4.8600	5.1500	28.9900	1.5100	1.4900	0.9400
440	5.0010	13.6416	5.5860	13.0242	8.9082	9.4276	0.4182	4.9572	5.2530	29.5698	1.5402	1.6390	1.0340
450	4.9107	13.3688	5.4743	12.7637	8.7300	9.2390	0.4266	5.0563	5.3581	30.1612	1.5710	1.8029	1.1374
460	4.7567	13.1014	5.3648	12.5084	8.5554	9.0543	0.4351	5.1575	5.4652	30.7644	1.6024	1.9832	1.2511
470	4.5365	12.8394	5.2575	12.2583	8.3843	8.8732	0.4438	5.2606	5.5745	31.3797	1.6345	2.1815	1.3763
480	4.2471	12.5826	5.1523	12.0131	8.2166	8.6957	0.4527	5.3658	5.6860	32.0073	1.6672	2.3997	1.5139
490	3.8854	12.3309	5.0493	11.7728	8.0523	8.5218	0.4617	5.4731	5.7997	32.6474	1.7005	2.6396	1.6653
500	3.4478	12.0843	4.9483	11.5374	7.8913	8.3514	0.4710	5.5826	5.9157	33.3004	1.7345	2.9036	1.8318

Table 5: Molar composition of the gas stream leaving the pyrolysis section for polypropylene [%]

T	H2	CH4	C2H4	C2H6	C3H6	C3H8	C4H10(ISO)	C4H8	C4H10(N)	C4H8	C4H6	C5H10	C6H12
400	9.0846	16.4499	2.1995	15.3848	22.5489	15.9091	0.8788	4.1668	0.8788	4.1668	0.0000	6.9615	1.3705
410	11.2478	15.6665	2.0948	14.6522	21.4751	15.1515	0.9251	4.3862	0.9251	4.3862	0.0000	7.5668	1.5228
420	13.1492	14.9205	1.9950	13.9545	20.4525	14.4300	0.9738	4.6170	0.9738	4.6170	0.0000	8.2248	1.6920
430	13.1275	14.2100	1.9000	13.2900	20.4525	14.4300	1.0250	4.8600	1.0250	4.8600	0.0000	8.9400	1.8800
440	13.3800	13.6416	1.8620	13.0242	20.0435	14.1414	1.0455	4.9572	1.0455	4.9572	0.0000	9.8340	2.0680
450	13.2039	13.3688	1.8248	12.7637	19.6426	13.8586	1.0664	5.0563	1.0664	5.0563	0.0000	10.8174	2.2748
460	12.8789	13.1014	1.7883	12.5084	19.2497	13.5814	1.0877	5.1575	1.0877	5.1575	0.0000	11.8991	2.5023
470	12.3936	12.8394	1.7525	12.2583	18.8647	13.3098	1.1095	5.2606	1.1095	5.2606	0.0000	13.0891	2.7525
480	11.7351	12.5826	1.7174	12.0131	18.4874	13.0436	1.1317	5.3658	1.1317	5.3658	0.0000	14.3980	3.0278
490	10.8895	12.3309	1.6831	11.7728	18.1177	12.7827	1.1543	5.4731	1.1543	5.4731	0.0000	15.8378	3.3305
500	9.8413	12.0843	1.6494	11.5374	17.7553	12.5271	1.1774	5.5826	1.1774	5.5826	0.0000	17.4215	3.6636

Table 6: Molar composition of the gas stream leaving the pyrolysis section for polystyrene [%]

T	H2	CH4	C2H4	C2H6	C3H6	C3H8	C4H10(ISO)	C4H8	C4H10(N)	C4H8	C4H6	C5H10	C6H12
340	0.2625	11.79041	11.4805	9.0178	18.2351	13.5342	0.0000	15.0014	3.8863	0.0000	0.0000	8.4205	8.3713
360	0.3179	12.1362	12.0078	10.8116	15.8962	14.3592	0.0000	16.1563	3.7037	0.0000	0.0000	7.7646	6.8464
380	0.3748	12.6255	12.6934	11.7538	14.8510	14.5160	0.0000	16.7256	3.5647	0.0000	0.0000	7.2363	5.6590
400	0.4342	13.24504	13.5311	12.0256	14.8229	14.1361	0.0000	16.8306	3.4570	0.0000	0.0000	6.8006	4.7169
420	0.4966	13.98868	14.5213	11.7439	15.6329	13.3029	0.0000	16.5490	3.3724	0.0000	0.0000	6.4343	3.9581
440	0.5626	14.85477	15.6690	10.9851	17.1620	12.0701	0.0000	15.9311	3.3048	0.0000	0.0000	6.1209	3.3396
460	0.6328	15.84462	16.9827	9.8001	19.3295	10.4721	0.0000	15.0095	3.2499	0.0000	0.0000	5.8487	2.8302
480	0.7074	16.96155	18.4731	8.2223	22.0799	8.5305	0.0000	13.8049	3.2043	0.0000	0.0000	5.6088	2.4072
500	0.7868	18.21014	20.1528	6.2740	25.3742	6.2589	0.0000	12.3302	3.1651	0.0000	0.0000	5.3944	2.0534
520	0.8712	19.59563	22.0359	3.9696	29.1835	3.6652	0.0000	10.5931	3.1300	0.0000	0.0000	5.2002	1.7556
540	0.9609	21.12337	24.1370	1.3191	33.4849	0.7545	0.0000	8.5979	3.0969	0.0000	0.0000	5.0217	1.5037

Table 7: List of compounds

Compounds		**Compounds**	
H2	hydrogen	**C4H10(ISO)**	iso-butane
CH4	methane	**C4H8**	1-butene
C2H4	ethylene	**C4H10(N)**	n-butane
C2H6	ethane	**C4H8**	2-butene
C3H6	propylene	**C4H6**	1,2-butadiene
C3H8	propane	**C5H10**	1-pentene
		C6H12	1-hexene

$$C_nH_m + (n + \frac{m}{4})O_2 \rightarrow nCO_2 + \frac{m}{2}H_2O \quad (1)$$

For each mole of a hydrocarbon of length n, n moles of carbon dioxide are generated.

The main reasons to perform an oxy-combustion process on such gaseous stream are:

- An incredible quantity of **heat** can be recovered with a combustion reaction: for instance, methane has a heating value of 55,4 MJ/kg. This heat can be recycled in the plant, to lower operational costs and enhance the thermal efficiency of the whole process: this is achieved by using the produced heat in the pyrolysis reactor, as well as heat exchangers in the plant, or for production of electric energy useful for the operation of the plant.
- The gas leaving the pyrolysis section is **useless**, while carbon dioxide can be easily stored and used for many purposes, for instance:
    - In a Fischer-Tropsch plant [36] to produce clean fuel
    - In the food industry, as a food preservative and to produce carbonated beverages
    - As a fire extinguisher
- Besides being useless, this gaseous current is potentially **dangerous**, if it comes in contact with oxygen in an uncontrolled environment. Burning it to CO_2 prevents uncontrolled explosion of the gases and, if stored correctly, takes the mixture out of its explosive limits.

The main problem with combustion is that it is a *runaway* reaction[1] so it must be carried out in very well controlled conditions not to lead to dangerous outcomes, obtaining the desired result. Of course, being in an oxy-combustion environment rather than a regular combustion one increases such risk, because the nitrogen contained in air would act as an inert and lower the temperature, but it would also

[1] *Runaway reactions* are highly exothermic reactions, characterized by very high reaction rates and a very high (and rapid) increase in temperature, so that they are very difficult to control. For instance, the reaction rate for the methane combustion (section 3.3) is 5.2461e+9 [s^(-1)].

increase *by around 4 times* the volume of the reactor, due to the air proportions between oxygen and nitrogen. Also, the presence of an inert gas acting as a *third body* could lower the temperature of the gases, lowering the possibility of heat recycling in the plant. Moreover, performing an oxy-combustion process nullifies the possibility of NO_x production, which can cause environmental pollution.

The reaction can be controlled by:

- **Injecting oxygen gradually**, to avoid explosion. In this sense, a controlled injection of oxygen only rather than air would be more precise for the lower volumes to be treated.
- **Cool down the reacting system** while the reaction takes place, to avoid crossing the maximum reactor admissible temperature.

1.5 Oxy-combustion reactor: KERIONICS Oxygen Transport Membrane system

A way of achieving a controlled oxygen injection by considering an oxy-combustion approach in the reacting system was provided by the company KERIONICS, which produces Oxygen Transport Membrane (OTM) systems.

An OTM system consists of membrane structures made of ceramic materials presenting mixed ionic-electronic conductivity (MIEC) which allows a 100% selective oxygen separation. This is due to the ability of MIEC materials to diffuse oxygen in the ionic form O^{2-} through the oxygen vacancies present in the material's crystal lattice

At high temperatures (>600 ºC), OTM technology has been demonstrated as an appealing option for the in-situ O_2 production in medium and small-scale applications. The main reasons are the *high O2 purity* that can be obtained and the *reduction in pure O2 production costs* of up to a 35% with respect to conventional technologies, such as cryogenic air distillation and Pressure Swing Adsorption (PSA) [37].

Furthermore, OTMs can reduce energy consumption and enhance overall plant efficiency due to the synergic thermal integration they provide [37]. At the same time, the use of OTMs result in more efficient and environmentally sustainable processes: this is due to the fact that by conducting combustions with pure O2, then only CO2 and H2O are generated and the capture and storage of the generated CO2 is enabled, along with a drastic reduction in CO2 emissions.

Typically, OTMs consider high permeating materials such as perovskites. The mineral itself named perovskite is a titanate with the formula $CaTiO_3$, but it is part of a *supergroup* of minerals having different compositions but the same, octahedral structure [38]. For a so called *stoichiometric* perovskite, the general formula is ABX_3, where A and B are large cations and X could be oxygen, but also fluorine (in fluoride perovskites) or large metalloids like nickel [38]. However, there are several non-stoichiometric perovskites with more complex formulas [38]. Amongst perovskites, the best performing material is $Ba_{0.5}Sr_{0.5}Co_{0.8}Fe_{0.2}O_{3-d}$, even if its low stability avoids its consideration for applications where reducing and CO_2-containing atmospheres can be met.

Other considered materials are the fluorites. Fluorites are a class of minerals with the formula MX_2: the common mineral fluorite is MX_2, but many compounds adopt this structure, like for instance BaF_2, PuO_2 and ZrO_2 [39]. They take a tetrahedral shape where the M element form a face-centered cubic (FCC) structure while the X element occupy the tetrahedral interstitial sites [39]. These materials present a higher stability when exposed to the mentioned environments; however, the lack of electronic conductivity result in poor permeation fluxes.

A solution is the use of composites or dual-phase materials, by combining a material presenting ionic conductivity with another presenting electronic conductivity, and both being stable under the considered environments, although stable MIEC materials can also be considered. There are many possible combinations of materials suitable for constituting a dual-phase material: ceramic-metal composites [40] [41] [42], fluorite-spinel [43] [44] [45], perovskite-spinel [46] and perovskite-fluorite [47].

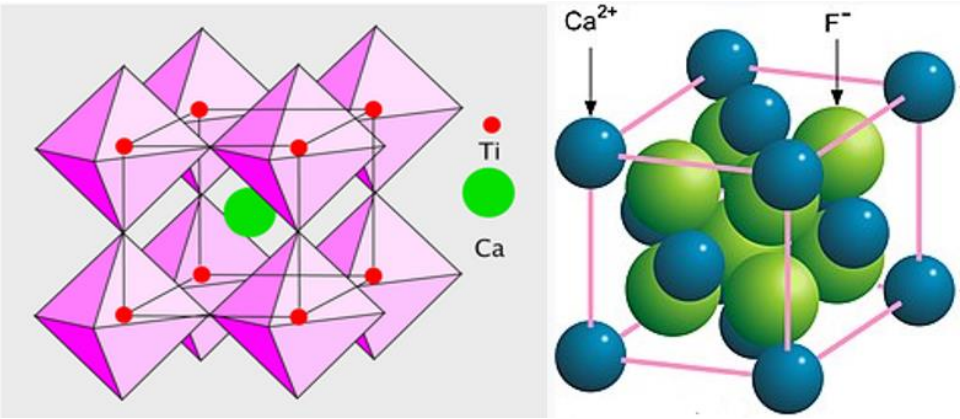

Figure 10: Structure of the ideal perovskite [38] and fluorite [48].

Oxygen contained in air undergoes an electrochemical process in contact with the membrane, so that it passes selectively through the membrane while letting nitrogen flow. The reaction mechanism is schematized below (Figure 11Figure 1): Usually when dealing with OTMs, the chamber where air passed is referred to as the *feed chamber*, while the *sweep* chamber is the one where any other gas passes.

The steps in the scheme represent the main resistances to the flux of oxygen [49]:

i. Oxygen *diffusion* from the feed stream to the membrane surface.
ii. Oxygen *adsorption* on the membrane surface at the feed side.
iii. *Dissociation* surface exchange reaction:

$$O_2 + 4e^- \rightarrow 2O^{2-} \quad (2)$$

iv. *Incorporation* of the oxygen ion into membrane crystalline structure.
v. Ion *diffusion through the membrane oxygen vacancies* (and electron counter-diffusion through electronic bands).
vi. O^{2-} *adsorption* on the membrane surface at the sweep side
vii. *Recombination* surface exchange reaction:

$$2O^{2-} \rightarrow O_2 + 4e^- \quad (3)$$

viii. Oxygen molecule *desorption* from the membrane surface
ix. Oxygen *diffusion* from the membrane surface to the sweep stream

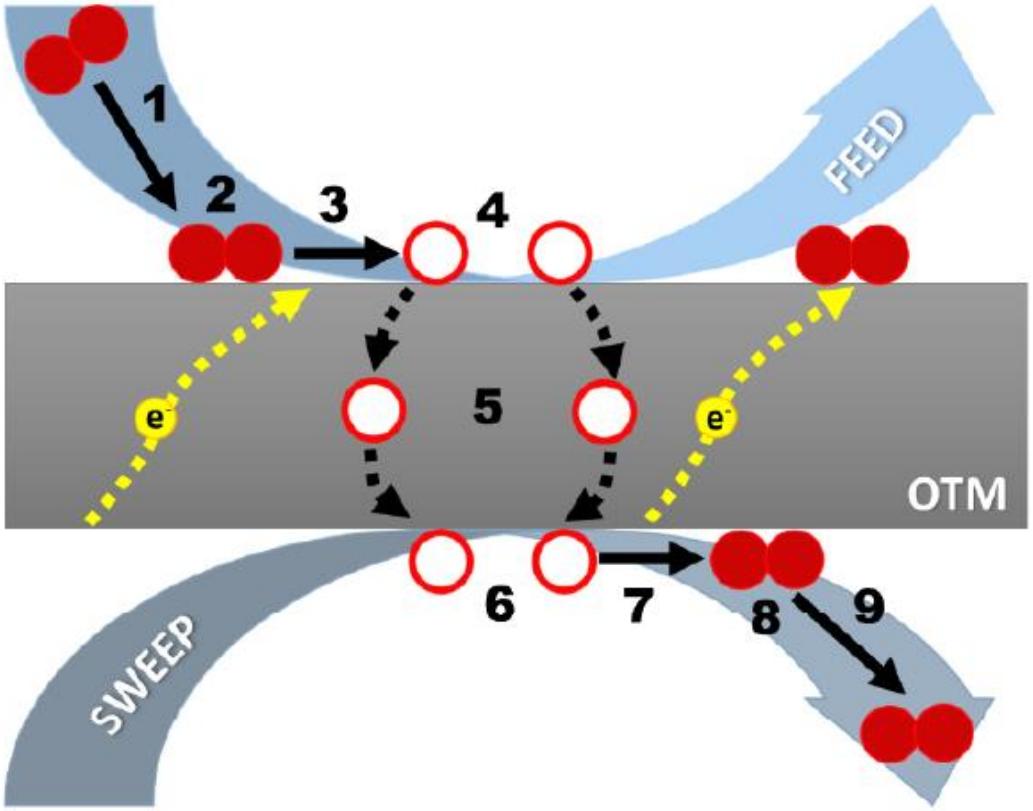

Figure 11: Simplified scheme of OTM process [50]

Coupling the quantitative information about the oxygen flux across the membrane with the one concerning the reacting system, it is possible to model an OTM oxy-combustion reactor.

1.6 Object of the thesis

For every kg of plastic processed, the iCAREPLAST plastic chemical recycle plant pyrolysis section produces between 5 and 20 kg of gases, depending on the type of processed plastic, and on temperature (Table 1: Weight yields for polyethylene pyrolysis [kg/kg of plastics], Table 2,Table 3). A safe, environmental-friendly, but also economically suitable solution must be implemented to dispose of this gas current and make a profit from it, in terms of energy recovery and value of the obtained products.

Oxy-combustion seems the most convenient solution, but it must be designed and controlled carefully, to monitor production and to avoid dangerous outcomes. A

membrane system is available for the task, to inject oxygen in the reacting system in a controlled way.

The former object of the thesis is to *model a membrane reactor* for the task and obtain information about conversion and temperatures of the currents leaving the system by *implementation of the model* in a script and *numerical integration*.

Also, once a precise, satisfyingly smooth computer model is created, it is possible to obtain quantitative results. The latter object of the thesis is to use this information to perform an *economic assessment* of the oxy-combustion section of the plant: it consists in a *parametric study* of the system, in order to identify the *working point* of the oxy-combustion section to obtain heat recovery and profit.

2. Materials, tools, and methods

A simplified scheme of the development of the thesis is depicted below (Figure 12):

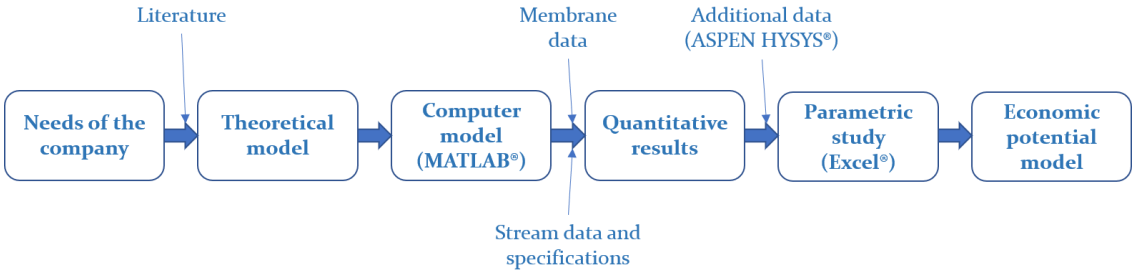

Figure 12: Scheme of the thesis

First of all, the model is created theoretically, with the support of articles and books found in literature about the thermodynamics and kinetics of the system.

Then, the theoretical model is implemented in MATLAB® to perform a numerical integration. The following data is used:

- Information about weight yields and composition of the gas stream leaving the pyrolysis section, available from iCAREPLAST (Table 1: Weight yields for polyethylene pyrolysis [kg/kg of plastics], Table 2,Table 3,Table 4: Molar composition of the gas stream leaving the pyrolysis section for polyethylene[%], Table 5, Table 6).
- Information about the membrane material and structure, available from KERIONICS (Table 8), such as:
    - Dimensions of the membrane
    - Heat conductivity and heat capacity of the membrane
    - Maximum allowed temperature and pressure
    - Dimensions of the whole structure
- Information about the oxygen transport mechanism, available from literature and applied to the specific membrane system.
- Thermodynamic values for the compounds involved in the system [51].
- Target values of conversion requested by iCAREPLAST.

Once the quantitative results are obtained from the software, these are coupled to new data, generated using ASPEN HYSYS®[2], related to other pieces of equipment in the oxy-combustion plant section. These data are used to perform a parametric study of the plant section, using Microsoft Office Excel®.

Eventually a theoretical model for the calculation of the economic potential is created, considering the whole study and the needs of the two companies.

[2] Aspen HYSYS® is a plant simulation environment where the performance of the plant can be evaluated, including various tools like fluid EoS packages and thermodynamics, various equipment simulation, but also calculation of investment cost and duties expenses.

3. Theoretical model of the OTM reactor

The aim is to obtain a mathematical model being:

- Based on solid hypotheses, to make the equations as slim as possible,
- Detailed in the definition of each term of the equations,
- As generical as possible, to comply with any given input data for the reactor.

3.1 Choice of the type of reactor

The information given by the company making the OTM system available is used to make a simplified reactor model. The membrane system that will be considered is constituted by *modules*: the structure of a single module is described below (Figure 13):

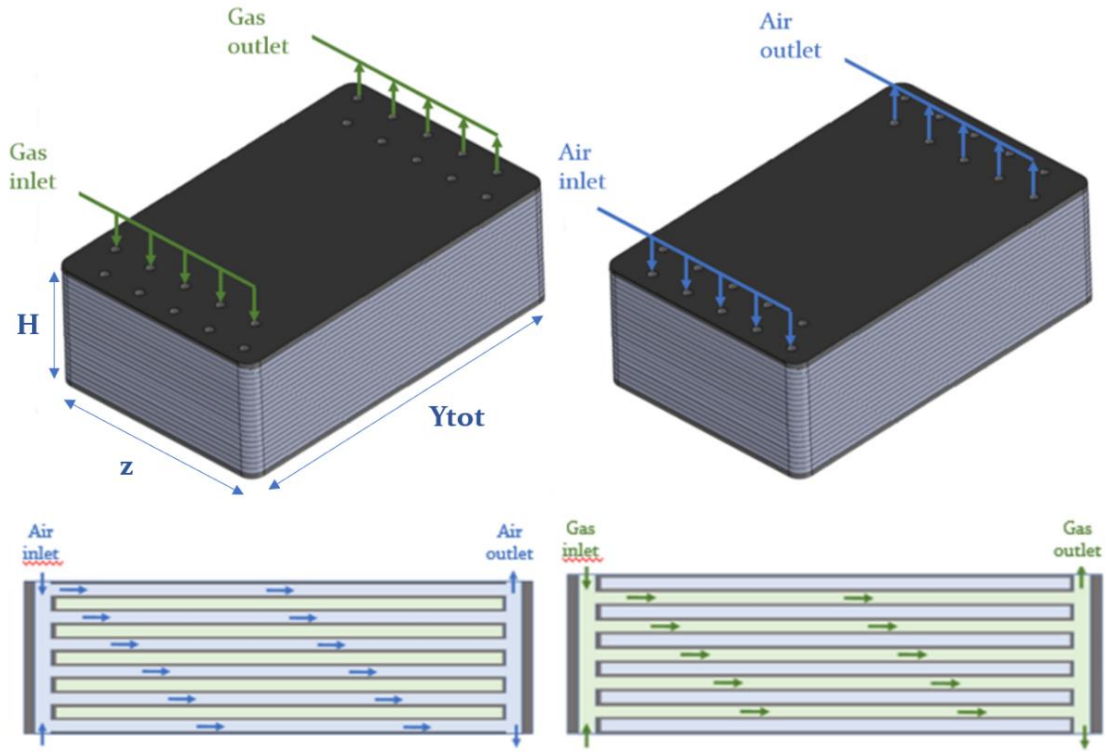

Figure 13: OTM module structure and dimensions

The OTM module is constituted by a series of superposed membranes, which divide the air flow from the pyrolysis gas flow This superposition makes sure that various *chambers* are created, between which each stream can divide and through

which it can flow, enhancing mass and heat transfer due to the much lower height of each chamber with respect to the whole module.

A simple scheme of the reaction environment (Figure 14), composed by two chambers separated by a membrane, will allow a better understanding of the choices taken in the modeling process, the definition of the dimensions of the chambers, and the structure of the membrane.

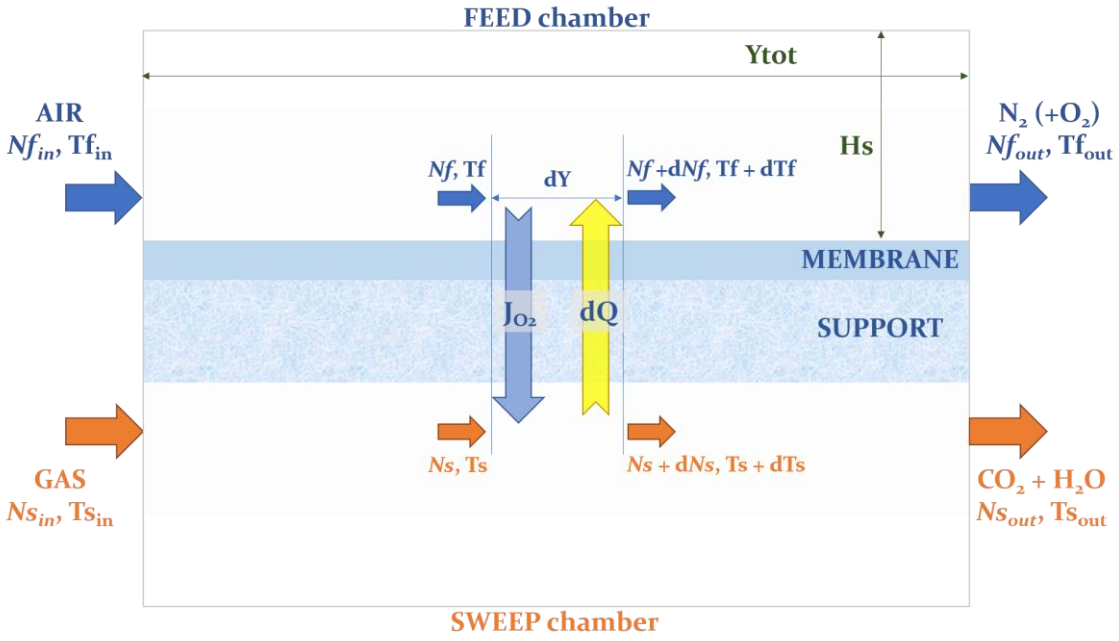

Figure 14: Scheme of the reaction environment and dimensions of a chamber (in green)

Quantitative values for the membrane are listed below (Table 8).

Table 8: Geometrical dimensions and structural properties of a chamber

Dimension	**Description**	**Value**
Hs	Height of the single chamber	2 [mm]
z	Width	25 [cm]
Ytot	Total length	25 [cm]
Tmax	Maximum temperature allowed	900 [°C]
Pmax	Maximum pressure allowed	8 [bar]
L	Dense membrane layer	20 [μm]
L_{supp}	Porous membrane layer	2 [mm]
k_{supp}	Heat conductivity of the porous support	5 [W/m/K]

Usually, OTM systems are composed by a thick membrane layer and a porous support layer (Figure 14).

If the overall structure of the module is considered, the total height H (Figure 13) will depend on the number of membranes in a single modulus:

$$H = \left(L + L_{supp}\right) * N_{membranes} + H_s * (N_{membranes} + 1) \qquad (4)$$

Where $N_{membranes}$ is the number of membranes in the reactor.

The height of a single chamber *Hs* is lower by 2 orders of magnitude than the total length *Ytot* and the width *z*. If the aim is to model just the part of the reactor that is sufficiently far from the inlet and outlet section (where some turbulence will occur due to the splitting of the stream and the change of direction of the fluid), we can assume for the sake of simplicity that the flow is homogeneous along the dimensions of the height *Hs* and the width *z*, and that it varies only along the coordinate of length *Y*.

In fact, the velocity along this coordinate will be much higher due to both the forced direction of the flow and the low transversal area. So, this is the only coordinate that will be investigated, using a *plug flow* model. The result will be a modified *Plug Flow Reactor* (PFR), with the difference that the contribution of mass transfer should be considered in the equations as well.

A co-current configuration is represented in the scheme (Figure 14): this is the one that is taken in consideration. A countercurrent configuration is discarded immediately due to the nature of the reactions involved, which require a good control of temperature. In fact the gas at the inlet of the reactor, characterized by high reaction rates when in contact with oxygen due to the maximum possible concentration of reagents, exchanges heat with the air that has already been heated up by combustion: a *hotspot*[3] can take place inside the reactor. The temperature in a hotspot can be higher than the maximum temperature allowed; moreover, it is

[3] A point at which the temperature inside the reactor has a maximum.

very difficult to control using the available variables (like the temperature of the air at the opposite side of the reactor, which is its inlet), and it can lead to runaway conditions in a very short time.

The mass and heat balance equation will be written by making a *steady state* balance in *an infinitesimal slice* of the reacting environment composed by the two chambers and the membrane, of length dY (Figure 14) [52]. Pressure drops are neglected in first approximation, to simplify the model.

3.2 Mass balance equations

If we state that *Ncomp* is the number of components in the gas stream, there will be *Ncomp + 2* mass balance equations to be built.

Considering the sweep chamber, the mass balance equations are so structured (t is the time coordinate):

$$\frac{dn_{s,i}}{dt} = N_{s,i} - \left(N_{s,i} + dN_{s,i}\right) + b_i dN_{ox,flow} + dN_r = 0, \quad [\text{mol/s}] \qquad (5)$$

Where:

- $n_{s,i}$ = moles of component i in the sweep chamber slice [mol]
- $N_{s,i}$ = stream of component i entering the sweep chamber slice [mol/s]
- $N_{s,i} + dN_{s,i}$ = stream of component i leaving the sweep chamber slice [mol/s]
- b_i = Boolean operator being
    - 0, if $i \neq$ oxygen
    - 1, if i = oxygen
- $dN_{ox,flow}$ = quantity of oxygen flowing per unit of time through the membrane [mol/s]. it is equal to:

$$dN_{ox,flow} = 2 * J_{O2} * z * dY, \quad [\text{mol/s}] \qquad (6)$$

Where J_{O2} is the oxygen flux across the membrane.

The system that has been considered in this work is made of a mixture of a perovskite, $La_{0.6}Sr_{0.4}Co_{0.2}Fe_{0.8}O_{3-\delta}$ (LSCF) and a fluorite, $Ce_{0.9}Gd_{0.1}O_{1.95-\delta}$ (CGO) dense membrane, with a porous support made of the same material. For this type

of membrane, the main resistances detected to the flux of oxygen are the surface reactions [53]. Due to this, the oxygen flux can be represented by a single formula [54]:

$$J_{O2} = \frac{D_v k_r \left(P'^{0.5}_{O_2} - P''^{0.5}_{O_2}\right)}{2Lk_f \left(P'_{O_2} P''_{O_2}\right)^{0.5} + D_v \left(P'^{0.5}_{O_2} + P''^{0.5}_{O_2}\right)}, \quad [\text{mol/m^2/s}] \qquad (7)$$

Where:

- J_{O2} = molar flux of oxygen per membrane surface
- D_v = oxygen vacancy bulk diffusion coefficient [m^2/s], with an Arrhenius type dependency on temperature[4].
- k_f, k_r = forward and reverse Arrhenius[4] reaction rate constants for the dissociation reaction (eq. (2))
- L = membrane thickness
- P'_{O2} = partial pressure of oxygen in the feed side [atm]
- P''_{O2} = partial pressure of oxygen in the sweep side [atm]

The values of the constant defining D_v, k_f, and k_r [55] are listed below (Table 9):

Table 9: Arrhenius constant values for oxygen transport membrane constants [55]

Arrhenius constant A*exp(-Ea/R/T)	**A**	**Ea [J/mol]**
D_v	1.01e-6 [m^2/s]	7.56e+4
k_f	9.21e+6 [m/atm^0.5/s]	2.68e+5
k_r	1.75e+15 [mol/m^2/s]	3.77e+5

The formula reflects the dependence of the oxygen flux on temperature, membrane thickness, and oxygen gradient difference between the two chambers. Due to the very low thicknesses usually involved, the temperature used in the equation is the

[4] An Arrhenius dependency on temperature takes the shape *k(T) = A*exp(-Ea/R/T)* where *A* is called *preexponential factor* and *Ea* is an *activation energy* while *R* is the universal gas constant [70].

air stream temperature. The whole flux is multiplied by 2 to consider the heat flux from above and below.

- dN_r = quantity of component *i* generated per unit time due to the reactions occurring. It is equal to:

$$dN_r = \left(\sum_{j=1}^{Nreact} \nu_{i,j} r_j \right) * A_t * dY, \quad [\text{mol/s}] \qquad (8)$$

Where

- N_{react} = number of total reactions
- $\nu_{i,j}$ = stoichiometric coefficient for component *i* in reaction *j*, positive if *i* is a product and negative if it is a reactant
- r_j = *j*-th reaction rate, function of gas temperature and composition[5] [mol/m^3/s]
- A_t = transversal area of the chamber = $Hs*z$

By inserting equations (6) and (8) in equation (5), and dividing by *dY*, we obtain:

$$\frac{dN_{s,i}}{dY} = b_i * J_{O2} * z + \left(\sum_{j=1}^{Nreact} \nu_{i,j} r_j \right) * A_t \qquad \text{for i} = 1...\text{Ncomp} \quad [\text{mol/s}] \qquad (9)$$

For the components in the feed chamber, oxygen and nitrogen, material balances are simpler because no reactions occur.

For oxygen:

$$\frac{dn_{f,O_2}}{dt} = N_{f,O_2} - \left(N_{f,O_2} + dN_{f,O_2}\right) - dN_{ox,flow} = 0, \quad [\text{mol/s}] \qquad (10)$$

Where:

- $n_{f,O2}$ = moles of oxygen in the feed chamber slice [mol]
- $N_{f,O2}$ = stream of oxygen entering the feed chamber slice [mol/s]

[5] A reaction rate is usually in the form $r = k(T)*f(\mathbf{C})$, where $k(T)$ depends on temperature in an Arrhenius fashion, and $f(\mathbf{C})$ is a function of the array of concentrations of the species in the system. A common shape for f is $\prod_{i=1}^{Ncomp} C_i^{\alpha_{i,j}}$ where $\alpha_{i,j}$ is the order of reaction *j* for the component *i*; it is called *power law*.

- $N_{f,O_2} + dN_{f,O_2}$ = stream of oxygen leaving the feed chamber slice [mol/s]

By using equation (6) and simplifying:

$$\frac{dN_{f,O_2}}{dY} = -J_{O2} * z \quad [\text{mol/s}] \qquad (11)$$

Since nitrogen does not flow nor react, its mass balance equation is trivial (N_{f,N_2} is the nitrogen stream in the feed chamber slice):

$$\frac{dN_{f,N_2}}{dY} = 0 \quad [\text{mol/s}] \qquad (12)$$

3.3 Reaction set: simplifications using the LHV

As stated before, the gas stream contains a great variety of compounds: all of these undergo combustion when in contact with oxygen, at very high reaction rates[6].

Since:

- the very interest of this thesis is to evaluate the quantity of carbon dioxide formed and the generated heat
- the speed and stability of the script has to be considered
- a single reaction set including all species is difficult to find in literature, and for the sake of the reliability of the model it is risky to combine different reaction sets coming from different studies – at different reaction conditions

The model is simplified by assuming a *pseudo-composition* of gases, where at the beginning only hydrogen and methane are present. This was done by converting the moles of the remaining hydrocarbons into their *methane equivalent* using their *lower heating value* (LHV)[7] [56]:

$$n_i^{CH_4,eq} = n_i \frac{LHV_i}{LHV_{CH_4}} \quad [\text{mol/s}] \qquad (13)$$

This way, the equivalent number of moles takes into account the number of carbon atoms in the chain *and* the heat that is generated from combustion. The total

[6] For instance, at T = 400°C the Arrhenius constant for methane oxycombustion is 8.8104*10^10 1/s.
[7] A measure of the heat produced by combustion of a mole of fuel.

amount of methane theoretically entering in the system is given by the sum of the methane equivalent for each compound, plus the actual amount of methane contained in the mixture.

The reaction set becomes much simpler. It is constituted by just two reactions: methane combustion [57] and formation of water from hydrogen [58]:

$$CH_4 + 2O_2 \rightarrow CO_2 + 2H_2O \quad (14)$$

$$H_2 + \frac{1}{2}O_2 \rightarrow H_2O \quad (15)$$

The values of the Arrhenius reaction constants are listed below (Table 10):

*Table 10: Arrhenius reaction constant of the reaction rates [57] [58]: [X] is the concentration of compound X, while k = A*exp(-Ea/R/T) (see note 4)*

Reaction	**Reaction rate**	**A**	**Ea**
Eq (14)	$k*[CH_4]^{-0.3}[O_2]^{1.3}$	8.3e+5 [1/s]	30 [kcal/mol]
Eq (15)	$k*[H_2][O_2]^{0.5}$	5.69e+11 [(m^3/kmol)^(1/2)/s]	1.468e+8 [J/kmol]

Regardless of the composition of the gaseous stream, the most abundant product is water: this requires a *separation section* downstream, for instance a flash unit for water condensation.

3.4 Heat balance equations

Two heat balance equations must be written, one on the sweep side and one on the feed side. T_s is the temperature in the sweep chamber while T_f the one in the feed chamber.

Considering the sweep side, the heat balance will be:

$$\frac{d\widehat{H}_s}{dt} = \dot{H}_s - \left(\dot{H}_s + d\dot{H}_s\right) + d\dot{H}_{ox,flow} - d\dot{Q} = 0, \ \text{[W]} \quad (16)$$

Where:

- $\widehat{H}_s$ = enthalpy in the sweep chamber slice [J]

- $\dot{H}_s$ = enthalpy flux related to the gas stream entering the sweep chamber slice. It can be expressed as:

$$\dot{H}_s = \sum_{i=1}^{Ncomp} N_{s,i} * h_i(Ts), \ \ [\mathrm{W}] \qquad (17)$$

Where $h_i(Ts)$ is the molar enthalpy of component i in function of temperature, which (if residual enthalpies are neglected, [52]) can be rewritten as:

$$h_i(Ts) = h_i(Tref) + \int_{Tref}^{Ts} c_{p,i}^{v}(T)\, dT_s, \ \ [\mathrm{J/mol}] \qquad (18)$$

Where:

  - T_{ref} = reference temperature (298 K)
  - $h_i(Tref)$ = enthalpy of formation of component i at the reference temperature at the gas state [J/mol]
  - $c_{p,i}{}^{v}(T)$ = heat capacity of component i, in function of temperature [J/mol/K]

- $\dot{H}_s + d\dot{H}_s$ = enthalpy flux related to the gas stream leaving the sweep chamber slice [W]. Using equations (17) and (18), the derivative in equation (16) is soon calculated:

$$d\dot{H}_s = \frac{\partial \dot{H}_s}{\partial T} dT + \sum_{i=1}^{Ncomp} \frac{\partial \dot{H}_s}{\partial N_{s,i}} dN_{s,i} = \sum_{i=1}^{Ncomp} N_{s,i} c_{p,i}^{v}(T) dT + dN_{s,i} h_i(Ts) \qquad (19)$$

- $d\dot{H}_{ox,flow}$ = enthalpy flux related to the oxygen flux across the membrane, expressed as:

$$d\dot{H}_{ox,flow} = J_{O2} * z * dY * h_{O_2}(Tf), \ \ [\mathrm{W}] \qquad (20)$$

- $d\dot{Q}$= heat transfer contribution, positive when flowing from the sweep chamber to the feed chamber, equal to:

$$d\dot{Q} = 2 * U * \Delta T * z * dY \ \ [\mathrm{W}] \qquad (21)$$

Where:

- U = global heat transfer coefficient [W/m^2/K], whose shape will be discussed below (see 3.5).
- $\Delta T = T_s - T_f$ = temperature drop across the membrane [K]

It is multiplied by 2 to consider the heat flux from above and below.

Using equations (9), (16), (17), (18), (19), (20) and (21) the heat balance is obtained:

$$\frac{dT_s}{dY} = \frac{J_{O_2} z \int_{Tf}^{Ts} c_{p,O_2}^{v}(T)dT - \sum_{i=1}^{Ncomp}\sum_{j=1}^{Nreact} \nu_{i,j} r_j A_t h_k(T_s) - U\Delta T z}{\sum_{i=1}^{Ncomp} N_{s,i} c_{p,i}^{v}(T_s)} \qquad (22)$$

Three main contributions can be distinguished in the equation: one related to the oxygen flux across the membrane, one related to the heat of reaction[8], and one related to the heat flux across the membrane.

The heat balance in the feed chamber has the same structure:

$$\frac{d\widehat{H}_f}{dt} = \dot{H}_f - \left(\dot{H}_f + d\dot{H}_f\right) - d\dot{H}_{ox,flow} + d\dot{Q} = 0, \quad [\mathrm{W}] \qquad (23)$$

Where:

- $\widehat{H}_f$ = enthalpy in the feed chamber slice [J]
- $\dot{H}_f$ = enthalpy flux related to the gas stream entering the feed chamber slice [W]
- $\dot{H}_f + d\dot{H}_f$ = enthalpy flux related to the gas stream leaving the sweep chamber slice [W]

Equations (17), (18) and (19) can be used also for the feed side: using equations (11) and (12), the heat balance becomes:

[8] Even if it comes with a negative sign, the contribution is positive: this quantity, called the enthalpy of reaction, is negative when the reaction is exothermic, because it accounts for the quantity of internal energy lost by the particles – therefore given to the environment.

$$\frac{dT_f}{dY} = \frac{U\Delta Tz}{N_{s,O_2} c^v_{p,O_2}(T_f) + N_{s,N_2} c^v_{p,N_2}(T_f)} \quad (24)$$

The contribution due to the oxygen flux across the membrane is not evident because the term $d\dot{H}_{ox,flow}$ was simplified with the term in equation (11). This shows that the flow of oxygen is taken into account in the sum of enthalpies in the denominator.

3.5 Heat flux contribution and global heat transfer coefficient shape

Equation (21) shows that the contribution due to the heat transfer between the chambers depends on the area between the two chambers, on the temperature difference and on *U*. Its shape depends on the three main resistances to the heat flux, which are:

- Forced convection in the sweep chamber
- Conduction across the OTM layer: due to the very low thickness of the dense membrane layer with respect to the porous one, the conductive resistance to heat flux through the dense layer is neglected.
- Forced convection in the feed chamber

The used formula for *U* is:

$$\frac{1}{U} = \frac{1}{h_s} + \frac{L_{supp}}{k_{supp}} + \frac{1}{h_f}, [\mathrm{W/m^2/K}] \quad (25)$$

Where:

- h_s = convective heat transfer coefficient of the sweep chamber [W/m^2/K]
- L_{supp} = thickness of the porous support [m]
- h_f = convective heat transfer coefficient of the sweep chamber [W/m^2/K]

The convective heat transfer coefficients in both sides (generically indicated as h) are calculated in first approximation using the Nusselt correlation for laminar flow on a flat plate [59]:

$$Nu_Y = 0.332 * ((Re_Y)^{1/2} * (\mathrm{Pr})^{1/3}) = \frac{h * Y_{tot}}{k_{mix}} \quad (26)$$

Where:

- $Nu_{,Y}$ = Nusselt number
- Re = Reynolds number, which is made explicit as:

$$Re_Y = \frac{\rho * v * Y_{tot}}{\mu_{mix}} \quad (27)$$

Where:

- ρ = gas density [kg/m^3]. It is calculated with this formula:

$$\rho = C_{tot} * PM_{mix} \quad (28)$$

Where:

- C_{tot} = total concentration of the gas phase [kmol/m^3]. It can be calculated using the ideal gas equation[9] or a more detailed equation of state[10] (EoS). For instance, using the Peng-Robinson EoS [60], at 400 °C and 8 bars, the total concentration is 22.3308 [mol/m^3], while using the ideal gas equation its value is 22.3351 [mol/m^3], so the difference is very low.
- PM_{mix} = molecular weight of the mixture[11].

- v = gas velocity [m/s]
- μ_{mix} = viscosity of the mixture [Pa*s]. It was calculated starting from the single component viscosities in function of temperature and using the Wilke model for mixture properties [61].

- Pr = Prandtl number, which is made explicit as:

$$Pr = \frac{\mu * cp_{mix}}{k_{mix} * PM_{mix}} \quad (29)$$

[9] The ideal gas equation is $PV = nRT$, so the concentration is $Ctot = n/V = P/R/T$

[10] It has the shape $Z = (PV)/(nRT)$ where, for a non-ideal gas, Z is different from 1.

[11] Mixture values are usually a sum of the value of the components, weighted by their molar fraction.

Where:

- cp_{mix} = heat capacity of the mixture[7] [J/mol/K]
- k_{mix} = heat conductivity of the mixture[7] [W/m/K].

After the definition of all the variables, it is possible to write down a script to incorporate the theoretical model.

4. Implementation in MATLAB® and numerical solution

If the mentioned hypotheses stand, to describe the entire system constituted by the two chambers and a membrane, only Ncomp + 3 equations are needed:

- *Ncomp* material balances, to describe the change in composition of the gas stream
- Just 1 material balance to consider the loss of oxygen from the air stream – the material balance on nitrogen can be neglected by imposing a constant flux of nitrogen equal to the inlet one
- 2 heat balances, on the sweep side and on the feed side, to account for the change in temperature of the currents.

This is an *ordinary differential equation* (ODE) system impossible to be solved analytically because each equation intrinsically depends on many variables and it is impossible to separate them.

That is the reason why it is implemented in the computing environment MATLAB®, which makes available several tools for numerical solution. Some of these are specifically meant to solve ODE systems, the *ODE solvers*[12].

4.1 Choice of the ODE solver

The ODE solvers have some differences, due to mainly two factors [62]:

- The *accuracy* required: this parameter significantly affects the computational time and effort of the program, because it has to do with the choice of the integration step. If a smooth function with low values of the derivatives is expected, then a lower accuracy solver could be chosen for the task.

[12] A numerical algorithm for the solution of a differential equation provides a value of the function *step by step*, in function of: the length of the step, the value of the function in the previous step, and the value of the derivative of the function. The simplest is the Euler method [63]

- The *stiffness* of the problem: in ODE systems, a stiff equation is a differential equation such that only certain numerical methods are stable, while others, simpler ones, are not – unless an extremely small step side is taken [63]. This is due to an abrupt change in shape of the function: the interval must be taken small enough to make this change smoothly.

ODE systems modeling integration in space (or time[13]) of chemical reaction mechanisms are usually constituted by stiff equations, due to the shape of the reaction rates, that can be many.

Moreover, as it was seen before, a combustion reaction is a runaway reaction: a small change in composition like controlled oxygen injection can lead to very high rates of reaction which lead to high, sudden increase in temperature.

Due to this, a solver for stiff problems with acceptable accuracy is used: *ode15s*. Also, a maximum step size is specified, to avoid loss of accuracy during the integration process.

4.2 Non-elementary reactions issue: the *modified* rate of reaction

A problem arises from the analytical shape of the material balances, which leads to unfeasible results if not correctly treated.

Total combustion reactions like the ones already shown above are *global reactions*, that is to say overall, experimentally visible formation of products and consumption of reagents. These are sums of several *elementary reactions* actually occurring in the reactor – for instance, in the case of combustion, a very radical chain mechanism takes place.

Considering a power law shape for the reaction rates, for elementary reactions the orders of reaction are equal to zero for the products and to the absolute value of the stoichiometric coefficient for the reactants. This is not true for global reactions,

[13] For instance, the system of equations for a batch reactor is very similar in shape, except that the variable of integration is time instead of a spatial coordinate.

whose orders of reaction for each species are calculated experimentally. This leads to the core of the problem, and to the solution proposed by Cuoci et al. [64].

To better understand the problem, an ideal batch reactor containing only two components, *A* and *B*, is considered: just a simple, non-elementary reaction occurs in it, $A \rightarrow B$. A balance on the component *A* is made, being α the order of reaction:

$$\frac{dC_A}{dt} = r(T, C_A) = k(T) * C_A^{\alpha} \quad (30)$$

In principle, α can also be less than 1, leading to the following numerical solution:

$$C_A = [C_{A0}^{1-\alpha} - (1-\alpha)kt]^{\frac{1}{1-\alpha}} \quad (31)$$

Where C_{A0} is the concentration of species A at time t=0. This means that the analytical solution allows C_A to be lower than zero after a certain instant, which is physically impossible.

Moreover, considering the specific system of equations to be solved, the oxygen flux term leads to a high oscillation of the reaction rates set of values. The numerical algorithm of the ODE solver leads to some sort of alternation of two moments, at each integration step:

- A step where oxygen is injected in the sweep chamber
- A step where oxygen is consumed by the reactants and temperature increases

This abrupt rise in the reaction rates may lead to negative concentrations of oxygen: the program registers that the reactant consumes "more oxygen than there actually is". The problem arises due to the presence of orders of reaction less than 1 and can be extended to more complex power law reaction rates.

This issue was solved by elaborating a *modified reaction rate*. Let us consider a power law of the *j*-th reaction with the formula:

$$r_j = k_j(T) \prod_{i=1}^{Ncomp} C_i^{\alpha_{i,j}} \quad (32)$$

For the numerical solution purposes, it can be substituted by:

$$r_j = k_j(T) \prod_{i=1}^{Ncomp} g_i(C_i, \alpha_{i,j}) \quad (33)$$

Where g is a function with the following shape:

$$g_i(C_i, \alpha_{i,j}) = \begin{cases} 1, & \alpha_{i,j} = 0 \\ C_i^{\alpha_{i,j}}, & \alpha_{i,j} \geq 1 \\ \xi C_i^{\alpha_{i,j}} + (1-\xi) C_{i,T}^{\alpha_{i,j}-1} C_i, & \alpha_{i,j} < 1 \end{cases} \quad (34)$$

Where $C_{i,T}$ is a constant representing a very low, almost considerable zero, concentration, and ξ is calculated as:

$$\xi = \frac{1}{2}\left[\tanh\left(\sigma \frac{C_i}{C_{i,T}} - \tau\right) + 1\right] \quad (35)$$

Where σ and τ are two appropriately chosen constants.

A comparison between the two solutions, obtained for the sample reaction scheme previously described, is shown below (Figure 15). When it approaches zero, using this numerical algorithm it becomes smaller and smaller by never being zero.

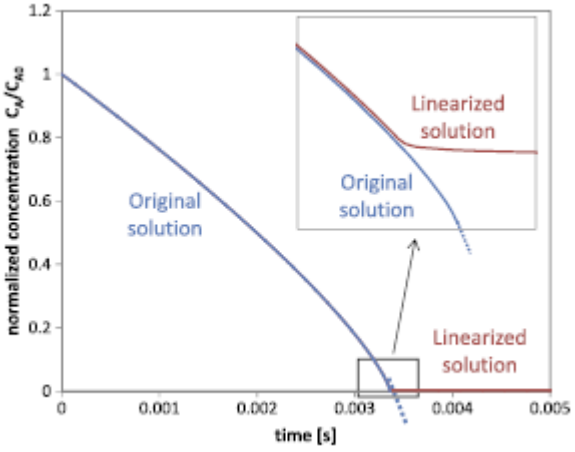

Figure 15: Comparison between the original solution and the modified reaction rate solution – here, linearized solution [64]

The MATLAB® function for the step-by-step calculation of the value of the reaction rate is reported in

Appendix A.

4.3 Results of the numerical model

In the MATLAB® code, there are mainly three types of variables:

- Some are *fixed* values, which are left unchanged at each integration. These are, for instance the geometrical dimensions of the membrane, the thermodynamic values of the components (or constants to calculate others), the constants to calculate the rates of reaction.
- Some are *independent variables*: these are used to make different simulations. More specifically, these can be:
    - The mass flux of the gas stream
    - The mass flux of the air stream – usually changed using a *multiplying factor* of the stoichiometric air necessary for combustion)
    - The composition of the gas stream
    - The inlet temperatures of the two streams
    - The inlet pressure of the two streams
    - The number of membranes in the module – usually changed in term of *number of fluxes* N_{fluxes} into which every stream is divided due to the presence of the membranes, considering that $N_{fluxes} = (N_{membranes} + 1)/2$ (see Figure 13).
- Some are *dependent variables*: these can be calculated at the inlet, like the equivalent methane quantity, or step by step to give the outlet results, like temperatures and compositions.

4.3.1 Qualitative analysis of the results

An example of integration can be seen below (Figure 16):

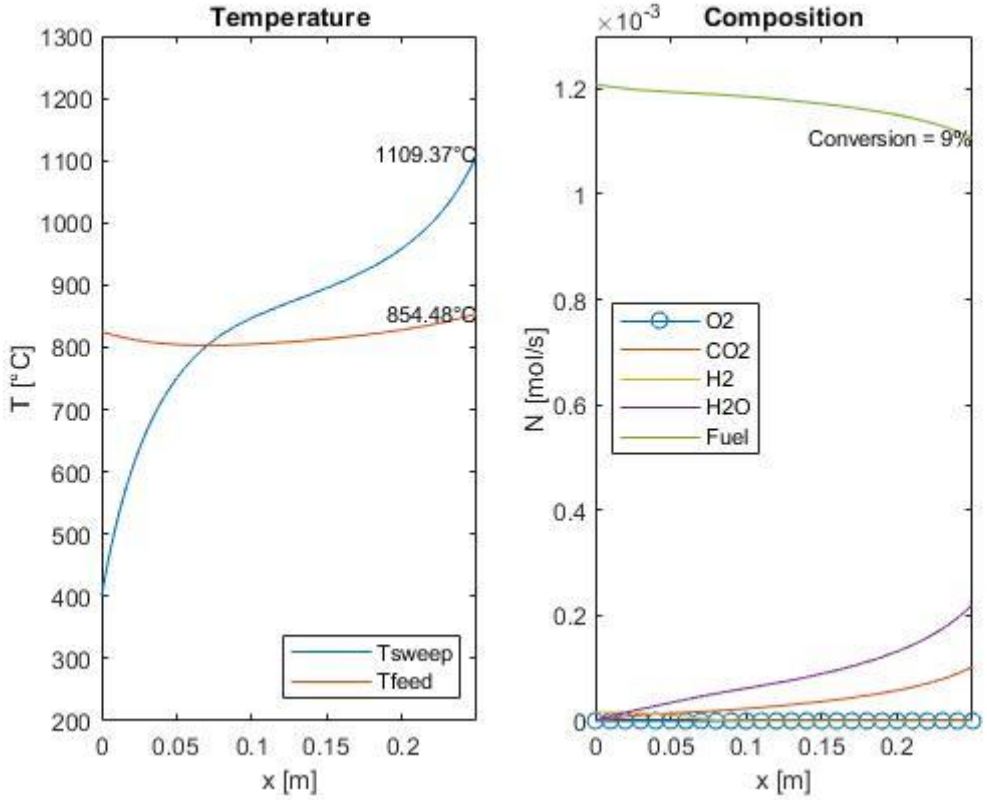

Figure 16: Example of temperature and composition profile in an OTM module, computed with the MATLAB® model

A first thing that can be noticed has to do with the **composition profiles**. While the fuel is being consumed, oxygen concentration stays close to zero: this means that as it passes through the membrane, it reacts with the gas stream. Also, water is the most abundant product of reaction – in agreement with the stoichiometry of the reactions.

Also, the **temperature profiles** can be considered qualitatively: air enters the reactor with a sufficiently high temperature to activate the membrane (around 800 °C) while the gas stream has an inlet temperature that is linked to the pyrolysis process (Table 1, Table 2, Table 3). In the first part of the reactor, heat exchange between the chambers prevails (the feed stream temperature lowers), while when combustion starts taking place quantitively, the temperature of the gases exceeds the temperature of the feed chamber, inverting the sense of the heat flux. Heat exchange across chambers appears quite limited, with respect to the heat produced by combustion.

Moreover, the runaway effect can be appreciated: the gas temperature rises becoming higher than the air temperature, the reaction rate increases (the slope of the fuel composition decreases) and the temperature increases even more, exponentially.

Due to this, an outlet temperature of more than 900 °C is registered, which is higher than the maximum temperature allowed in the module structure (Table 8). Nevertheless, the registered conversion does not even exceed 10% - it is not weird, reminding that the length of the reactor is 25 cm. This leads to a more accurate reactor design process.

4.3.2 Stability of the numerical model

As mentioned above (see 4.1), the set of equations is stiff: the reactions are very fast and temperature rises in an exponential fashion, therefore stability issues arise when trying to obtain feasible quantitative results.

The main, most evident case of instability regards the integration step. The maximum integration step can be chosen between the options for an ODE solver. If a too large integration step is chosen, the results can change abruptly (Figure 17). This is due to mainly two reasons.

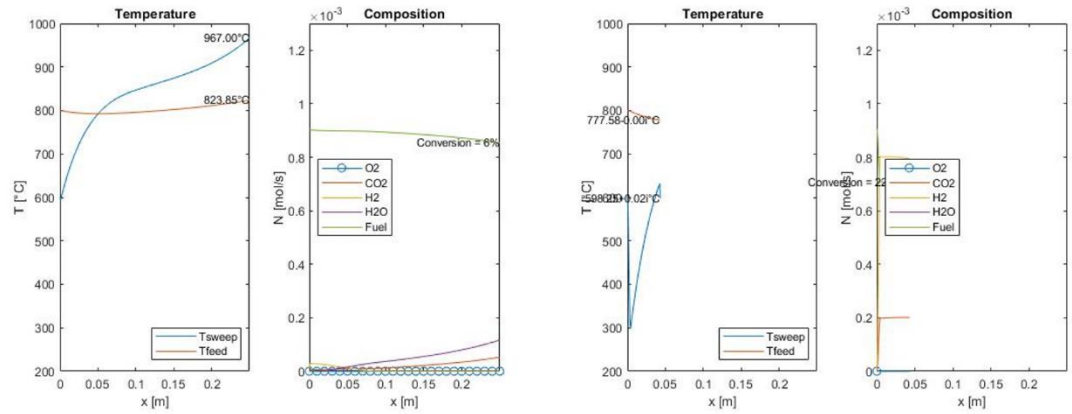

Figure 17: Two different results of the same simulation, at integration steps equal to 0.0001 and 0.01 m, respectively

The first refers to the calculation of thermodynamic variables. When sweep temperature exceeds certain (unfeasible) values like 1100 °C, the numerical solver

gives impossible values of concentrations as output, like negative values or imaginary values.

This is due to the shape of the viscosity and heat conductivity polynomial functions of temperature, experimentally derived in certain temperature ranges, which decrease when temperature increase. When the temperature exceeds such ranges, the values become negative, and the Wilke model [61] having square roots cannot fit negative values.

This problem could be solved calculating average values of viscosity and heat conductivity. The problem is that they could no longer be representative of the reacting environment due to the strong change in composition – from fuels ranging from C1 to C6 to carbon dioxide and water. Anyway, the coefficients are properly calculated in the ranges of temperature of interest for the reaction: it can just be said that if this problem arise, the operating temperature for the reacting system is unfeasible anyway.

The second refers to the computation of the concentrations inside the reactor. In fact, despite the modified rate of reaction function (see 4.2), if the integration step is not sufficiently low, negative concentrations of oxygen can be computed by the solver, which bring about complex functions of temperature and concentrations due to the shape of the reaction rates.

The instability issue is much less evident when reaction conditions are milder (Figure 18). Nevertheless, it is important to always have a high precision even if the results are not of use for the final operative conditions, to have inputs on how much the inlet conditions have to be changed to reach feasible results; the first simulations may be time consuming due to the very low integration step, but it is easier to get to the desired result and *then* increase the integration step to have similar results in much less time.

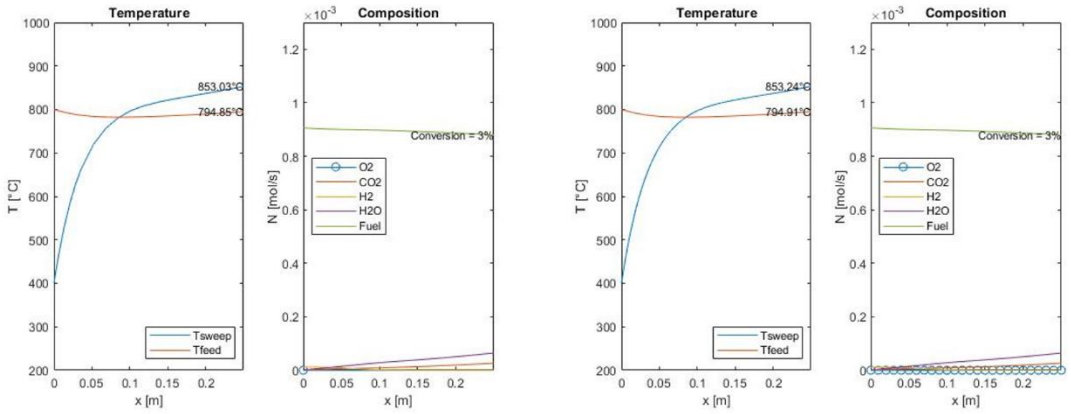

Figure 18: Two different results of the same simulation, at integration steps equal to 0.0001 and 0.1 m respectively, at milder reaction conditions

4.4 Adiabatic multi-stage reactor with intermediate heat recovery: design and implementation in MATLAB®

In the design phase, a compromise must be taken between:

- The desired target conversion (around 95%) for the reasons seen above.
- The maximum temperature allowed in the OTM module, due to its mechanical and thermal resistance (Table 8).
- The CAPEX for the total equipment in the plant section, given by the total amount of equipment purchased.

A possible design configuration is proposed: an *adiabatic multi-stage reactor* with *intermediate cooling*. The idea is simple:

- Several OTM modules are put in series, whose number depends on the desired overall conversion.
- At the outlet of each module, the temperatures of the two streams are brought to their inlet values, leading to a *progressive heat recovery* from the system – for instance, with the production of steam to be recycled in the plant.
- This operation should be accompanied by a subsequent *pre-heating of air* entering each step, or else the reaction will not proceed due to the membrane deactivation at low temperatures (Figure 19):

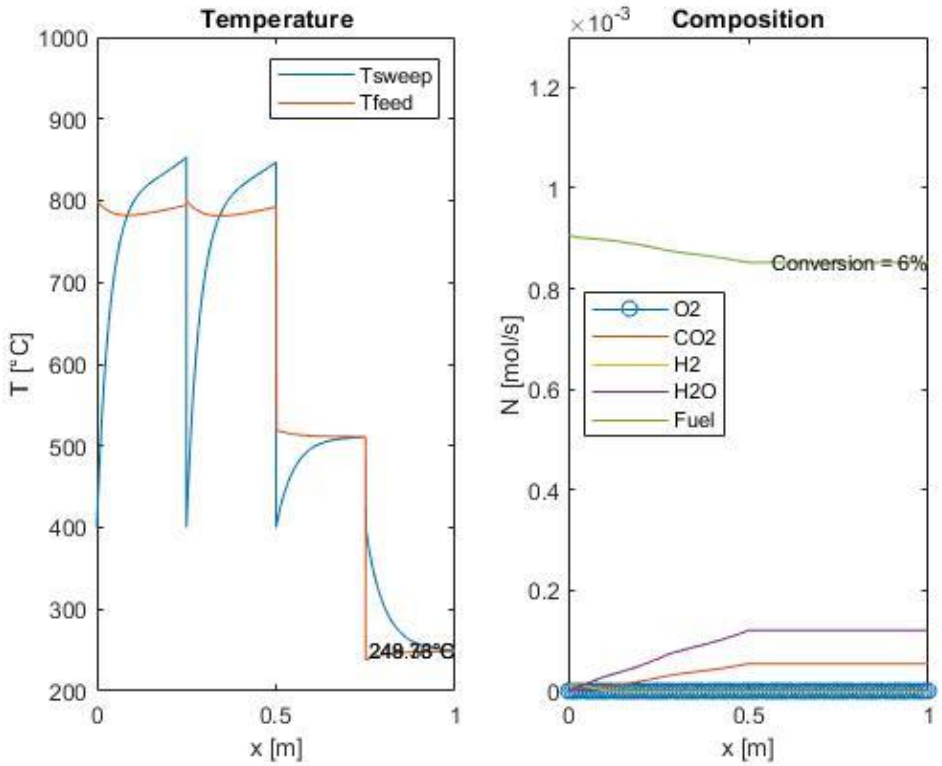

Figure 19: Loss of activity of the reactor if a pre-heating system is not implemented

Usually, this kind of solution is implemented for different types of reaction, for instance in the case of exothermic reactions, whose kinetics increase with temperature but whose equilibrium conversion is higher at lower temperature[14], such as the production of ammonia [65]. Here the case is different: the aim of the configuration is to limit the excessive increase in temperature because reaction rates are so high that the equilibrium conversion is not limited.

A scheme of the multistage configuration with intermediate heat recovery is depicted below (Figure 20):

[14] The equilibrium constant of a reaction increases with temperature for endothermic reactions and decreases as temperature increases for exothermic reactions (van 't Hoff equation [52])

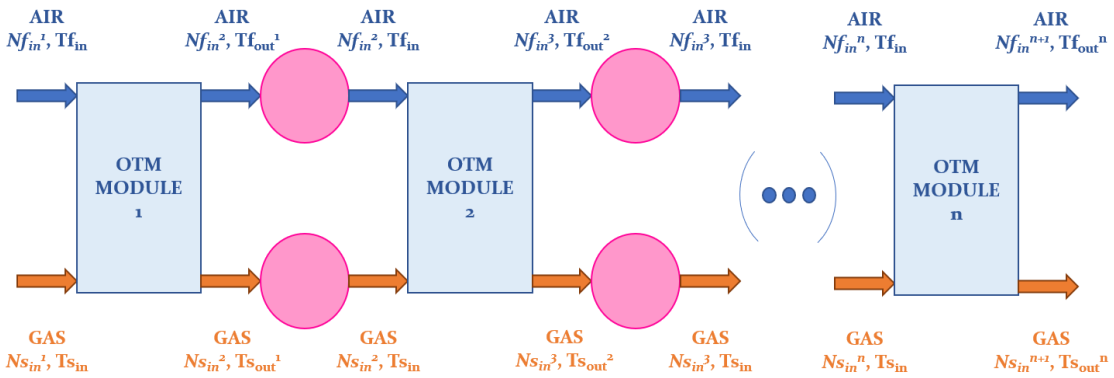

Figure 20: Multistage OTM system scheme

This way, the single unit would not be stressed by too high temperatures and an appreciable conversion can be reached, leading to a higher economical value and safety of the outlet current.

Numerically speaking, this is done by:

- Coding a *for-cycle* for the resolution of the ODE, which performs the integration as much times as the number of the desired OTM modules in series – or just *stages*.
- As inlet values for every integration:
    - The outlet composition of the last stage is chosen.
    - The temperature would be equal to a specific inlet temperature for each stage – for instance, it can be equal to the inlet temperature of the first stage.
- After the integration at each step, two quantity of energy are calculated:
    - One is the *heat generation*, from the cooling stage of the gas current.
    - One is the *heat need*, to heat the air stream, which should be brought back to a temperature at which the membrane is active.

  The difference between these two energy quantities is the *net heat* that can be recovered from the system, if properly designed.

An example of multiple stage integration can be appreciated below (Figure 21):

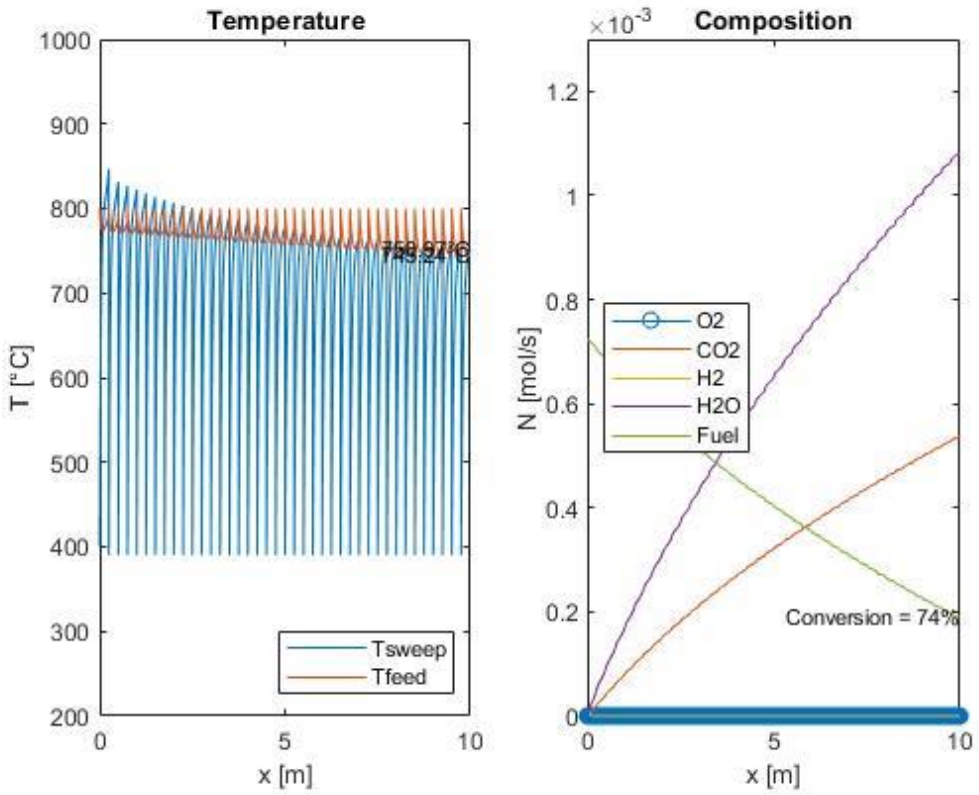

Figure 21: Example of temperature and composition profile in an OTM module series, computed with the MATLAB® model

For instance, in this simulation, the number of membranes has been regulated to obtain a maximum temperature inside the reactor lower than 900 °C, and 40 OTM modules were put in series, of a total length of 10 m (Table 8). The evolution of the composition has a shape that is very similar to the one of a single reactor, but in the single stages a variation in the reaction rate can be appreciated. The temperature rise at each stage becomes smaller, because the reaction rate increases always less due to consumption of the reagents.

Since the model gives feasible and useful numerical results, these can be used to perform a deeper parametric study of the oxy-combustion section.

The algorithm for an adiabatic multi-stage reactor with intermediate cooling used in MATLAB® is reported in Appendix B.

5. Parametric study of the oxy-combustion section and economic considerations

5.1 Definition of the problem

The object of investigation of a profit study on the whole system is to understand how some values of economic interest for the oxy-combustion section change in function of some appropriately chosen variables. The final aim is to draw the possibility to obtain a *combination of variables that lead to the lowest possible expense with the highest possible profit from the reaction*.

In this sense, it is important to define what brings profit and what causes expense in this section of the plant:

- As said in section 1.4, profit can be made in terms of produced carbon dioxide (denoted by conversion with respect to the total amount of gases) and of recovered heat from the combustion of gases.
- Expenses derive from:
    - Capital expenditure (CAPEX): this is made of all the equipment cost, including the OTM system, the compressors needed, the heat exchangers needed (function of the number of stages).
    - Operating expenditure (OPEX): this is made of all the energy required and the cooling or heating utilities required.

Moreover, a remark should be made on safety, as the set of chosen variables should allow the reactor to work at temperatures and pressures lower than the maximum allowed values.

5.2 Definition of the variables

The variables of interest for the study are of two types: there are *independent variables* and *dependent* ones. The former are the ones that can be manipulated to get to the desired combination of the latter for the economical optimization of the plant. All of these are chosen between all variables for their influence in the economic balance of the plant section.

The considered independent variables are:

- The *number of stages*.
- The *refrigeration temperature* (T_{refr}) that is the inlet temperature of the gas stream at each step.
- The *number of membranes* (or the number of fluxes into which each of the two stream is divided).
- *Air inlet temperature* at each stage (*TinOx)*.
- *Air pressure* – or equivalently, the pressure difference across the membrane.
- *Air quantity* with respect to the stoichiometric quantity of air with respect to the reactions, defined through a multiplication factor *a* which corresponds to:

$$a = \frac{{N_{f,O_2}}^{tot}}{{N_{f,O_2}}^{stoichiometric}} \quad (36)$$

Usually, an excess of air is used, around 2-3 times the stoichiometric amount.

The dependent variables of interest are:

- The *fuel conversion*: defined as:

$$\chi_{fuel} = \frac{{N_{s,fuel}}^{in,tot} - {N_{s,fuel}}^{out,tot}}{{N_{s,fuel}}^{in,tot}} = \frac{{N_{s,CO_2}}^{out,tot}}{{N_{s,fuel}}^{in,tot}} \quad (37)$$

- The *maximum temperature in the reactor*
- The *net produced heat*, the difference between *heat generation* and *heat need* (see 4.4), defined as:

$$NetHeat = Heat_{gen} - Heat_{need} = \sum_{k=1}^{Nstages} N_{s,k}^{tot} \int_{Trefr}^{T_{s,k}^{out}} cp_{mix,s}(T)dT - \sum_{k=1}^{Nstages} N_{f,k}^{tot} \int_{T_{f,k}^{out}}^{TinOx} cp_{mix,f}(T)dT \quad (38)$$

- The overall *inlet duties*. Neglecting pressure drops and heat losses in piping from the pyrolysis section to the oxycombustion one, the gas stream reaches the first OTM module at the outlet conditions of the pyrolysis section.

Therefore, the accounted inlet duties are just compression and subsequent pre-heating of the air stream to bring air to the reactor inlet conditions, Q_{comp} and Q_{heat} respectively – calculated with Aspen HYSYS® for each case.
The simulations are made considering that air is taken from the external environment at 25 °C and 1 atm.
It is important to remind that compression duties and heat duties are not provided in the same form: in fact, the compression duty is provided in the form of electrical energy and heat duty can be provided via heat exchange with a current of hot gases. Nevertheless, they are summed for a comparison with the amount of energy produced by performing the oxy-combustion process: the quantity of energy produced in the reaction is then transferred to the required units to be used.

Before considering the variation of each dependent variable with every independent variable, it is better to make a first regression on the air pressure.

5.3 Air pressure effect

The effect of air pressure was investigated due to the theorical dependence of the oxygen flux on the oxygen partial pressure difference across the membrane (eq. (7)). Experimental results actually show a very low dependence on this variable (Figure 22). This is due to several causes:

- Oxygen permeation increases (very little) with air pressure, but not in a linear way: it has an asymptotic, self-stabilizing behavior. This can be appreciated at lower pressures.
- Introducing an air excess with respect the stoichiometric quantity of air needed for the required values of conversion (see 5.2), oxygen exhaustion is avoided and the value of the partial pressure of oxygen remains more stable in the length of the reactor.

The driving force of oxygen permeation is being *more affected* by the absence of oxygen in the sweep chamber, which is consumed as it enters (Figure 21).

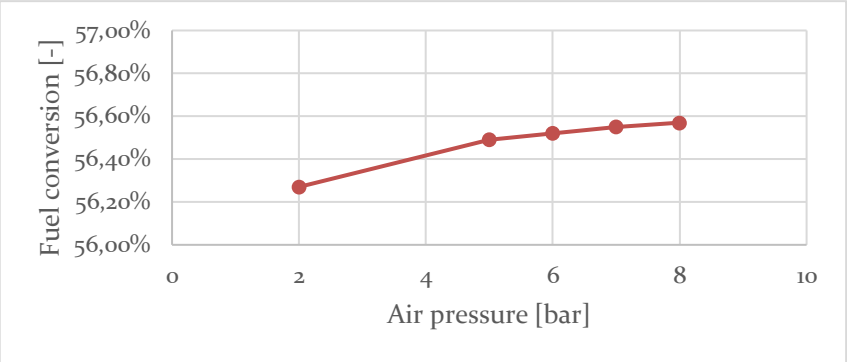

Figure 22: Dependence of the fuel conversion on air pressure.

In a very high pressure range, the fuel conversion changes of few percentage points. A very small change is registered also for the maximum temperature in the reactor and the net produced heat.

Using the Peng-Robinson EoS fluid package in Aspen HYSYS®, being the gas very rarified in the considered conditions (very close to an ideal gas, see 3.5), the results show that the total inlet duty for the air current also does not depend significantly on pressure[15] (Figure 23):

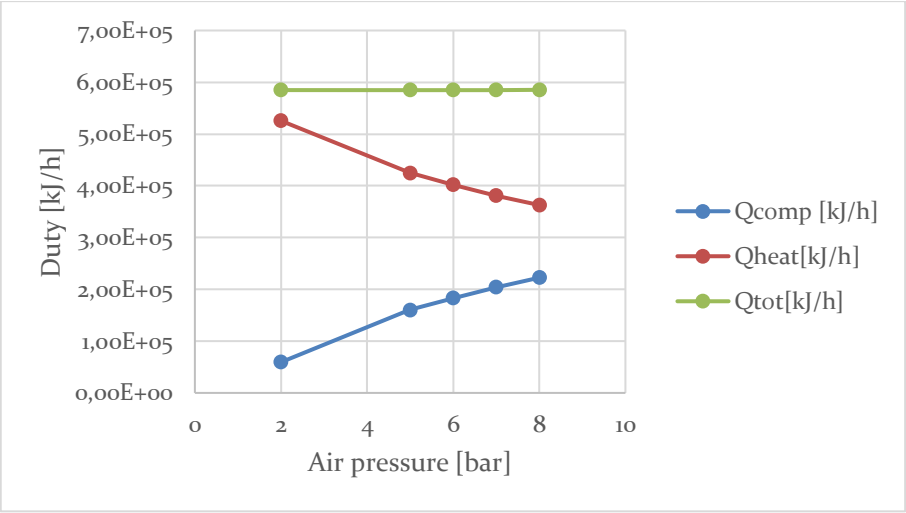

Figure 23: Dependence of compression duty, heating duty and total inlet duty on air pressure

In fact, compression also causes a rise in temperature, higher and higher as the outlet pressure rises: the heating duty lowers accordingly.

[15] The enthalpy of an ideal gas does not depend on pressure but only on temperature.

The costs related to compression are usually the highest in terms of CAPEX, so these results are of great help for the overall economic balance. In fact, due to such considerations, the choice of the air stream pressure can be taken according to considerations related to pressure drops along the plant section only.

5.4 Parametric study on the dependent variables

5.4.1 Fuel conversion

Fuel conversion defines the convenience of the whole process: not only the quantity of produced heat depends on the degree of combustion, but the storage conditions for the gas stream become easier and it also produces an economical value (see 1.4).

Predictably, it increases with the number of stages, as the reaction has the chance to proceed (Figure 24):

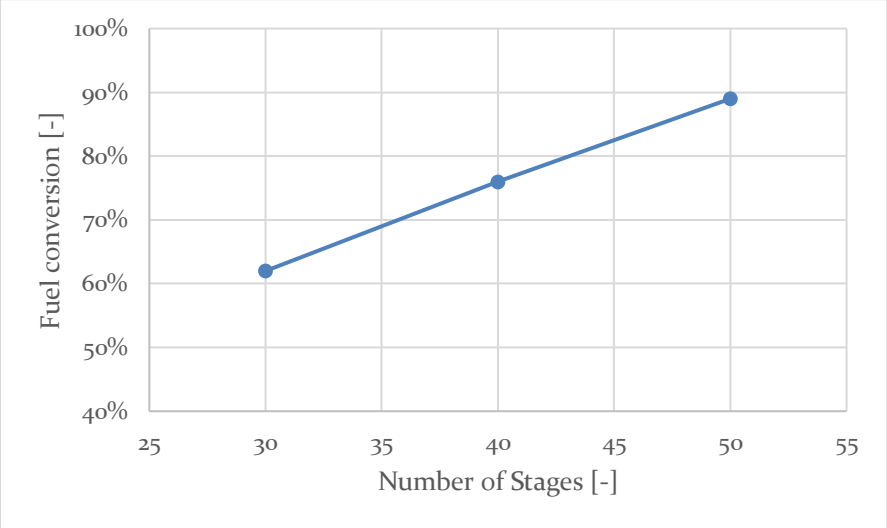

Figure 24: Dependence of the fuel conversion on the number of stages

The overall fuel conversion also increases linearly with the refrigeration temperature (Figure 25: Dependence of the fuel conversion on the refrigeration temperature):

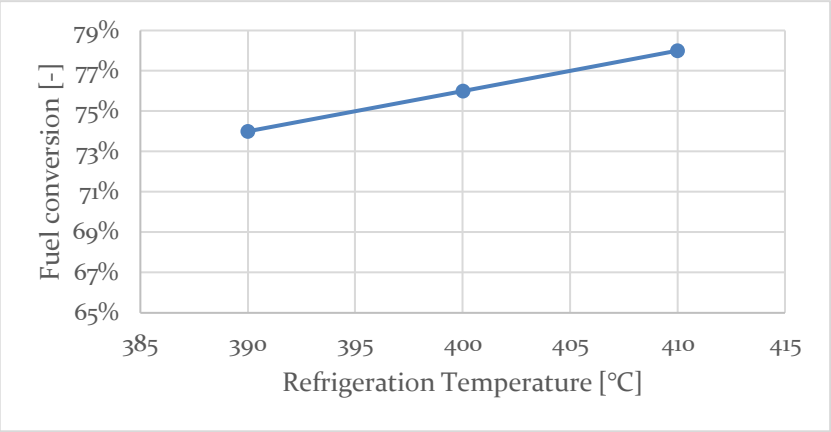

Figure 25: Dependence of the fuel conversion on the refrigeration temperature

This happens because of the *kinetic control* of the system: thermodynamic restrains on conversion due to the exothermicity of the reaction are negligible, so what counts is the higher reaction rate at higher refrigeration temperatures. Also, a higher temperature in the sweep chamber increases the heat transfer between the two chambers, so that oxygen permeation increases. Nevertheless, it can be noticed that the proposed system leads to a very *efficient control* of a combustion reaction, which has very high reaction rates.

A higher number of fluxes leads to lower molar fluxes in each chamber, at equal total molar flux: it means lower concentrations and lower reaction rates, but it also brings about lower space velocities (more time for the reaction to take place) being the reaction rate very high anyway. Therefore, the fuel conversion increases (Figure 26).

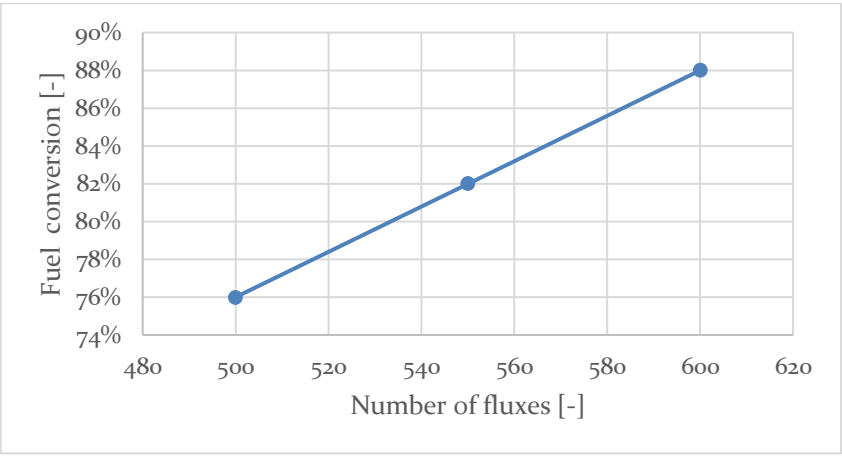

Figure 26: Dependence of the fuel conversion on the number of fluxes

It increases with the air inlet temperature, due to higher oxygen fluxes across the membrane (eq. (7)) (Figure 27):

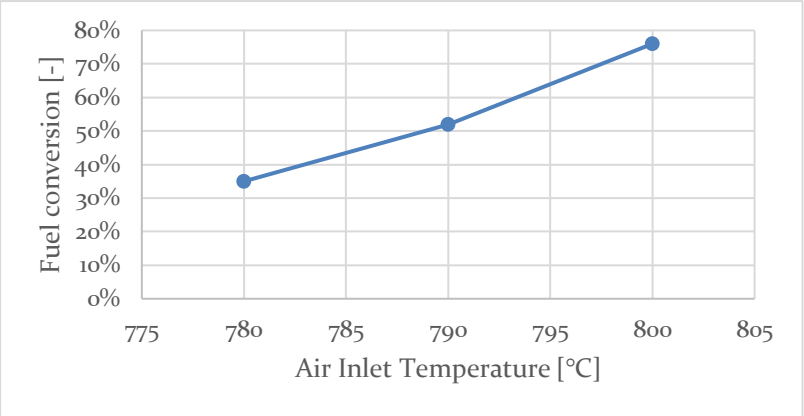

Figure 27: Dependence of the fuel conversion on the air inlet temperature

It appears that the relation between the fuel conversion and the air quantity is different than the one with the air pressure: it increases significantly increasing the molar flux of the air stream (Figure 28).

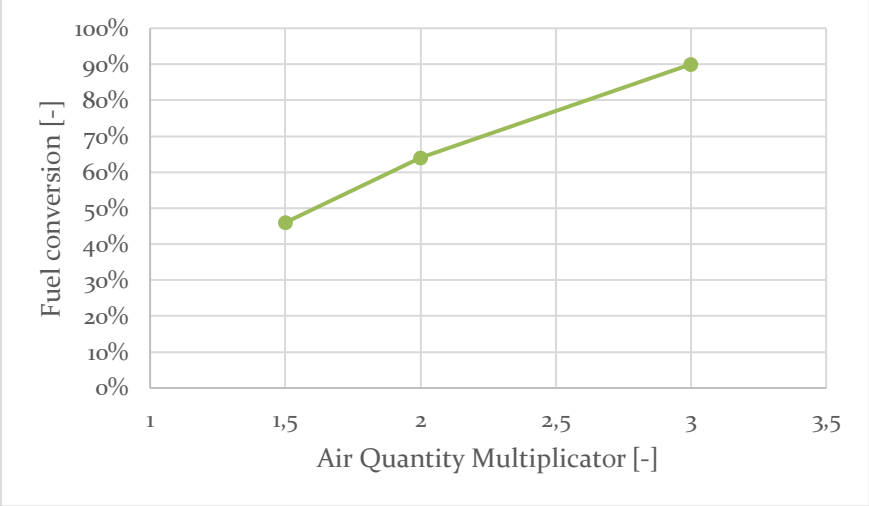

Figure 28: Dependence of the fuel conversion on air quantity

A higher molar flux of oxygen in the feed chamber increases the oxygen concentration drop across the membrane (the driving force of oxygen permeation) in the whole length of the reactor: oxygen exhaustion is reduced, leading to higher oxygen diffusion rates at the same total reactor length. It also increases the heat transfer across the membrane in the first part of each module, increasing the reaction rates faster.

5.4.2 Maximum reactor temperature

If the fuel conversion is satisfactory but the maximum temperature reached in the reactor is higher with respect to the maximum allowed (i.e. 900 °C, see Table 8), then the overall configuration is to be discarded. This parameter is of outmost importance for safety issues.

As it can be noticed, at equal length of the modules in series, the highest temperature inside the reactors is registered at the outlet of the first reactor, in the sweep chamber (Figure 29):

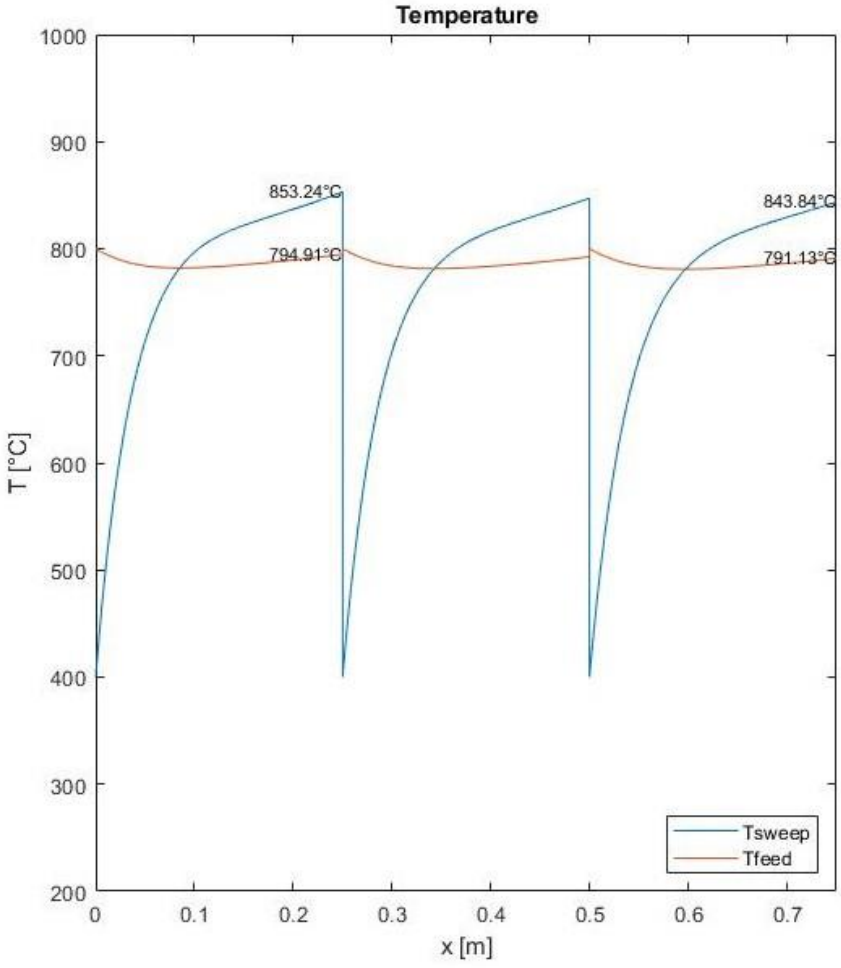

Figure 29: Example of few stages to indicate the maximum reactor temperature

The highest temperature is registered in the sweep chamber due to the fact that, as discussed above, at a certain point the combustion heat brings the gas stream temperature to exceed the air stream temperature.

At the outlet of the first reactor the temperature is the highest because, at the same conditions, the reaction rate is the highest, due to a higher concentration in reactants. Therefore, this value does not depend on the number of stages nor on the refrigeration temperature, which are variables that only affect the overall output.

A rule of thumb is: *what makes conversion increase also lets the maximum reactor temperature increase, except for the number of stages and the refrigeration temperature.* Predictably, a higher quantity of burnt fuel causes a higher rise in temperature, so the effect caused on the fuel conversion by the number of fluxes, the air inlet temperature and the air quantity can be appreciated also in the maximum reactor temperature, with the same shape (Figure 30,Figure 31,Figure 32):

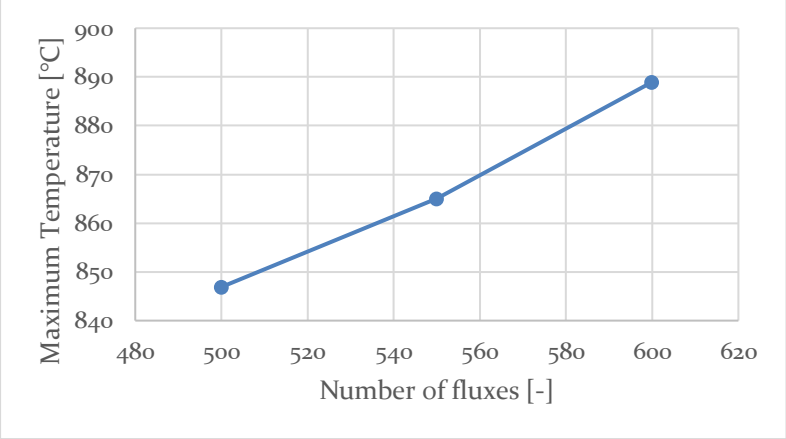

Figure 30: Dependence of the maximum reactor temperature on the number of fluxes

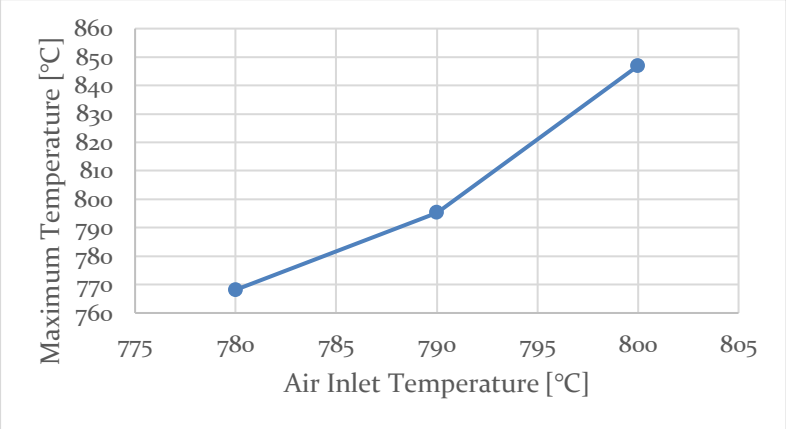

Figure 31: Dependence of the maximum reactor temperature on the air inlet temperature

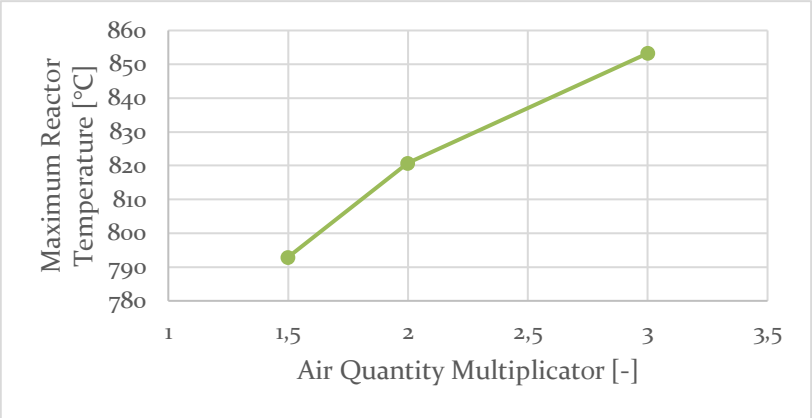

Figure 32: Dependence of the maximum reactor temperature on air quantity

5.4.3 Heat generation, heat need and net heat

In an ideal plant configuration, the exact quantity of net heat obtained from the difference between progressive cooling of gases and pre-heating of air between each step can be recycled in other parts of the plant. It could be used to compensate compression and heating of air at the inlet of the oxy-combustion section, or if it still exceeds it can be used in the pyrolysis section.

Fortunately, the heat generation is always higher than the heat need, because of the lower temperature difference between the outlet temperature of the air stream at each reactor and the air inlet temperature – always in a range between membrane activity and maximum temperature allowed in the reactor.

As the number of stages increase, this net difference increases as well due to higher oxy-combustion conversions achieved, pointing out a lower rise in temperature of the air stream with respect to the gas stream as the reaction proceeds (Figure 33):

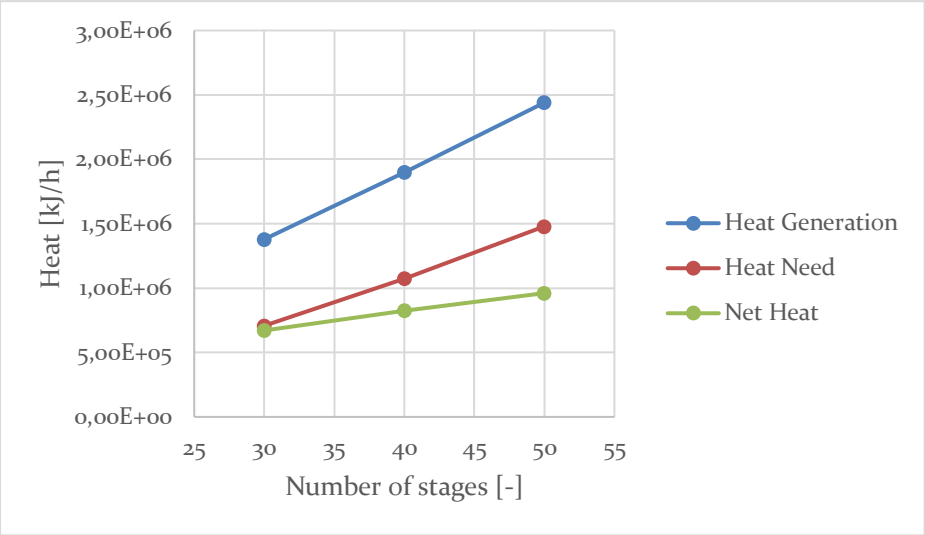

Figure 33: Dependence of net heat on the number of stages

If the refrigeration temperature is higher, the heat generation is lower due to less cooling of the gases: it is interesting to notice that the heat need is also lower, due to higher temperatures reached in the reactor, therefore a lower duty is required to pre-heat the air entering the system. The resulting difference increases as the refrigeration temperature increases (Figure 34): it brings about an advantage with respect to cooling fluid pumping and cooling equipment dimension.

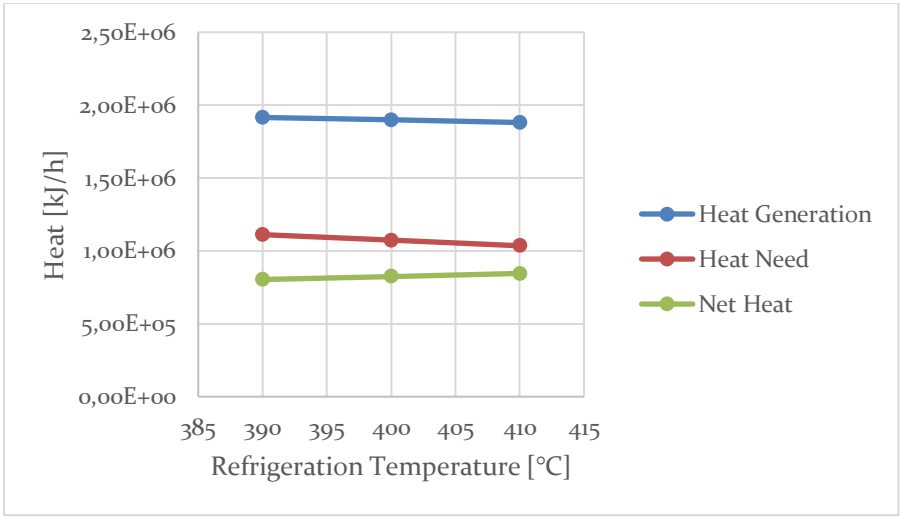

Figure 34: Dependence of heat generation, heat need and net heat on refrigeration temperature

The heat generation increases with the number of fluxes due to the higher combustion rate, and the heat need slightly decreases for the higher temperatures kept in the feed chamber thanks to heat exchange: therefore, the net heat increases (Figure 35):

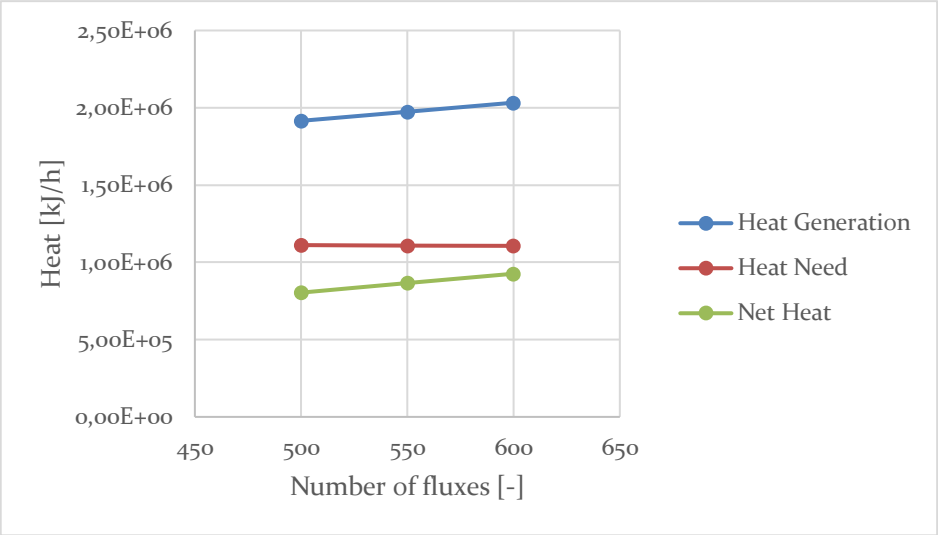

Figure 35: Dependence of heat generation, heat need and net heat on the number of fluxes

In general, *the variables that should increase the heat need have a positive effect on the combustion rate, too*: this causes a positive effect on the heat generation, with a higher slope with respect to the heat need increase. In fact, while the heat need increase is low and linear[16], the heat generation increase is high and exponential.

In this sense, it is interesting to notice that, unexpectedly, choosing a higher air inlet temperature, the net heat increases (Figure 36): this is due to the fact that the rise in heat generation due to more efficient and rapid combustion is higher than the rise in heat need, to pre-heat air to the chosen temperature.

[16] A shortcut formula to calculate the heat duty for a heat exchanger is $Q = F*cp\_av*\Delta T$; if an average heat capacity is calculated (cp_av), it linearly depends on the total molar flux F and the temperature difference ΔT.

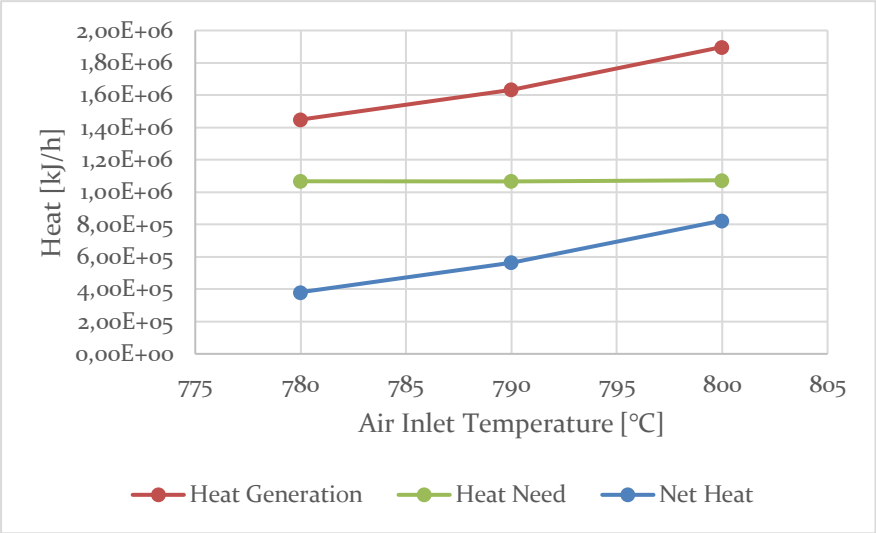

Figure 36: Dependence of heat generation, heat need and net heat on the air inlet temperature

The same can be stated for what concerns the air quantity (Figure 37): the heat generation increase due to a higher combustion rate is higher than the heat need increase due to a higher molar flux to be heated up, so the difference is always positive and grows with the air quantity multiplicator.

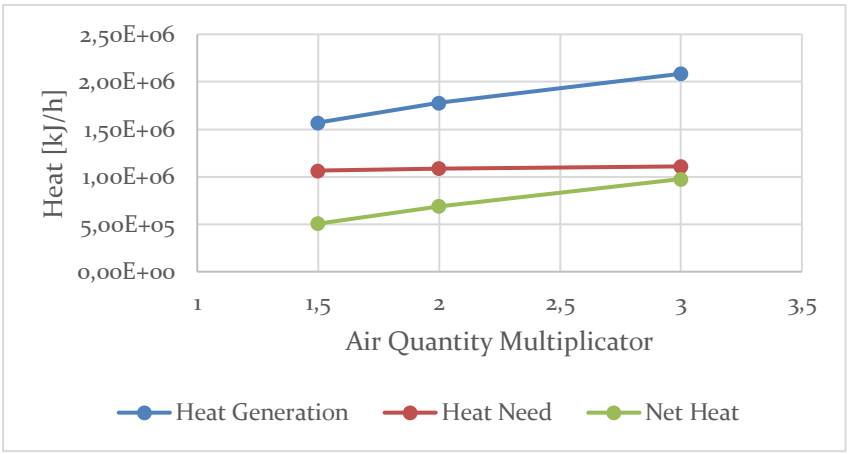

Figure 37: Dependence of heat generation, heat need and net heat on the air quantity multiplicator

5.4.4 Overall inlet duty and comparison with net heat

As stated above, compression and heating of air from the atmospheric conditions to the conditions of interest are very expensive operations in terms of CAPEX and OPEX, so it is very important to take them into account in a generical parametric

study of the system. Neglecting the dependence on pressure, the only two variables that have an influence are the air inlet temperature and the air quantity.

Predictably, the overall inlet duty increases with the inlet temperature, due to the increase of the pre-heating duty (Figure 38), and with the air quantity – still for the preponderant contribution of the heating duty (Figure 39).

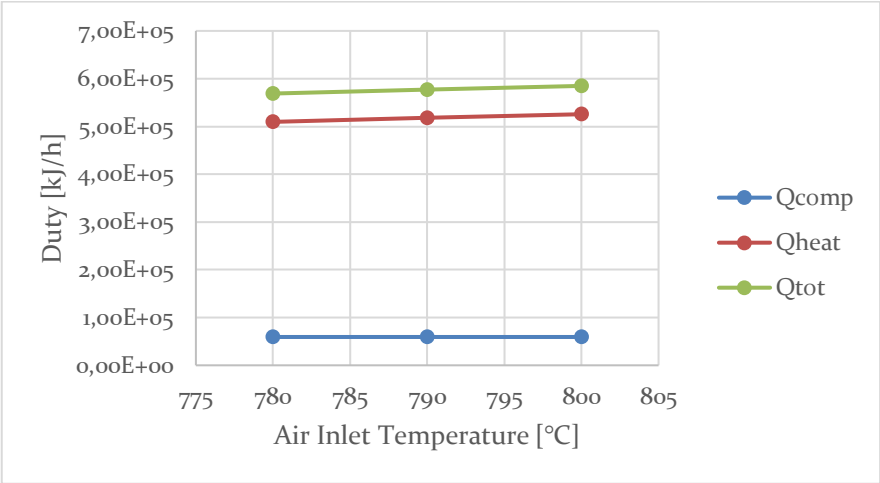

Figure 38: Dependence of the inlet duties on the air inlet temperature

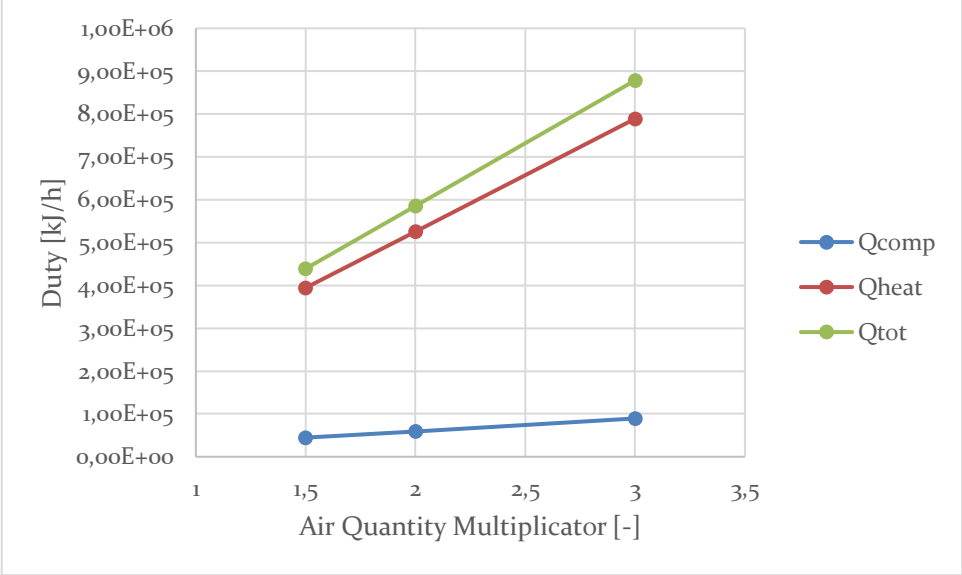

Figure 39: Dependence of the inlet duties on the air quantity multiplicator

In an outlook of heat integration, it is interesting to perform a comparison with the net production of heat at different conditions. The next two plots bring an important piece of information for the final design of the system as a whole.

The former is computed with respect to the air inlet temperature, these results are obtained (Figure 40):

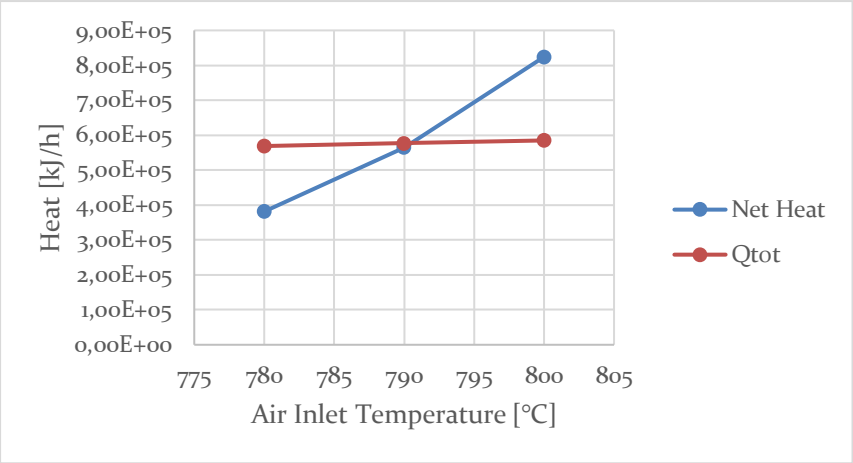

Figure 40: Comparison between total inlet duty and net heat production at different air inlet temperatures

At an increase in the air inlet temperature corresponds a higher increase in net heat with respect to the increase in total duty.

The latter is a comparison between the two values at different air quantities, but considering the number of fluxes as well (Figure 41):

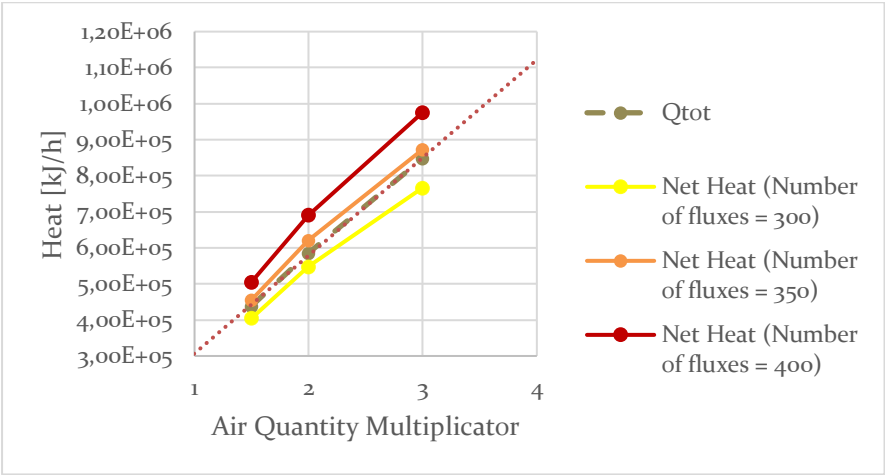

Figure 41: Comparison between total inlet duty and net heat production at different air inlet temperatures and number of fluxes

The overall inlet duty grows with the air quantity multiplicator, and so does the net produced heat but with a different fashion: the most interesting thing to notice though is that by increasing the number of fluxes, the net heat curve shifts above the duty line.

From these two plots, it can be deduced that *there is an optimal combination of values that lead to an overall positive energy profit*. This information is exploited in the elaboration of the economic model.

A last reflection has to be made in a *scale-up* outlook, to design a proper reactor for a final objective pilot plant.

5.5 Scale up and parallel reactors configuration

The parametric study shown above reflects the variation of the variables of interest using inlet values *per kg of pyrolyzed plastic* (Table 1: Weight yields for polyethylene pyrolysis [kg/kg of plastics]). To reach the capacity of the objective pilot plant considered in the iCAREPLAST project (see 1.3), considerations about the conversion of a much higher quantity of plastic to be treated in the plant must be made.

If, hypothetically, the plant configuration remains unchanged, as well as inlet temperatures and pressures and the air quantity multiplicator, a higher quantity of plastics (meaning a higher quantity of treated gas) lets the outlet values of interest drop significantly.

Fuel conversion has a non-linear, sudden drop (Figure 42):

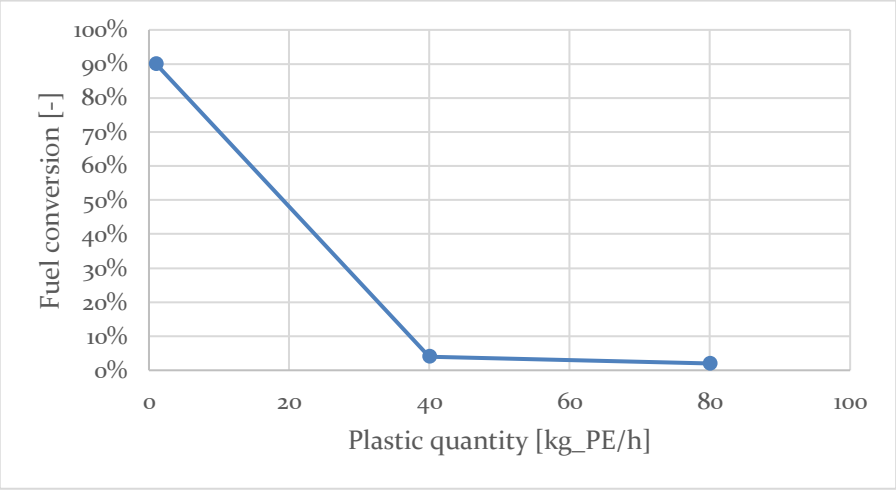

Figure 42: Dependence of fuel conversion on the pyrolyzed plastic amount

The overall inlet duty grows linearly with a very high slope, in comparison with the net heat produced (Figure 43):

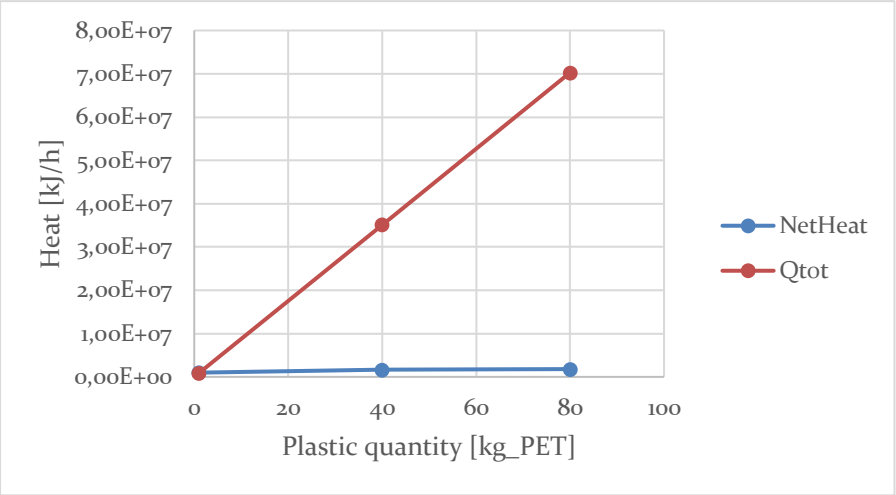

Figure 43: Dependence of overall inlet duty and net heat production on the pyrolyzed plastic amount

This means that the reactor structure as well as the inlet conditions must be changed to obtain suitable values of conversion and heat production.

A combination of various measures can do the job:

- Pushing thermodynamic conditions, like air inlet temperature and/or refrigeration temperature
- Changing the reactor configuration, by increasing the number of fluxes and/or the number of stages

While it is difficult to reach the desired combination of output values, the reactor undergoes a higher level of mechanical and thermal stress than before. To scale up the plant, further considerations must be made, one of these being the *depth* of the reactor.

The height of the reactor is given by the number of chambers composing it, while the length is given by the length of a single step multiplied by the number of stages (see 3.1). One thing that can be changed is the overall z dimension (Figure 13), by putting more reactors *in parallel*.

If we assume that the reactors are *tightly and securely connected*, this configuration can be translated, in terms of oxygen transport, in an *increase of the available surface*: the totality of the reactors can be considered as a single reactor having a depth dimension z equal to:

$$z = z_{module} * u \quad (39)$$

Where z_{module} is the depth of a single OTM module (Table 8) and u is the quantity of parallel reactors.

The fuel conversion and, of course, the maximum reactor temperature grow linearly with the quantity of reactors in parallel (Figure 44 andFigure 45):

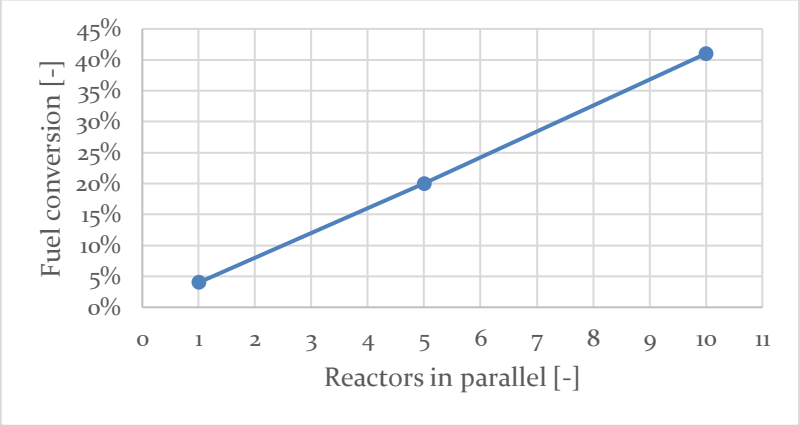

Figure 44: Dependence of fuel conversion with the quantity of parallel reactors

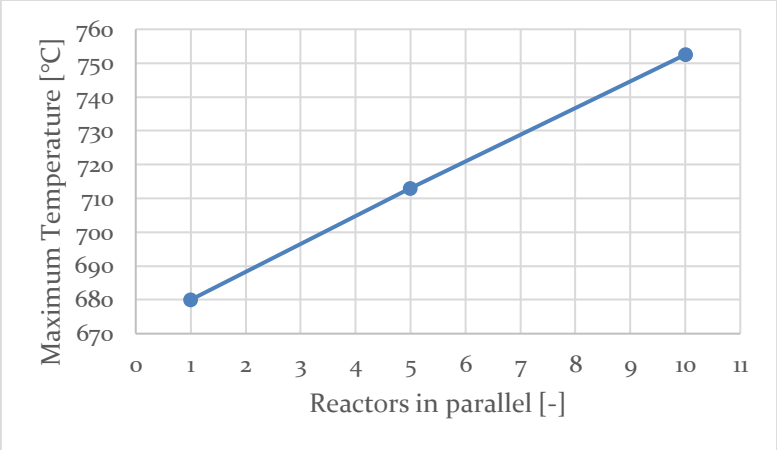

Figure 45: Dependence of maximum reactor temperature with the quantity of parallel reactors

The most interesting thing that can be noticed is that while the heat generation term increases linearly, the heat need term decreases linearly, so the net heat produced has a very high growth rate with the quantity of parallel reactors (Figure 46).

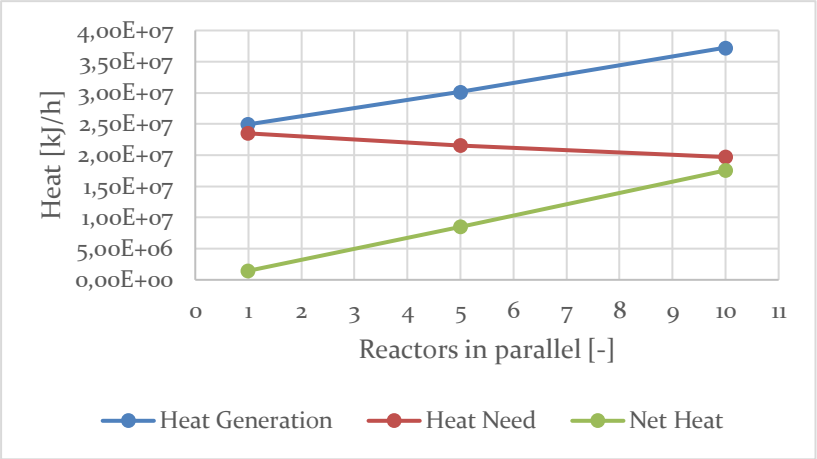

Figure 46: Dependence of heat generation, heat need, and net heat produced on the quantity of parallel reactors

The overall inlet duty remains unchanged because it only depends on the quantity of air to be treated and on its thermodynamic conditions: using such configuration, the net heat can exceed the overall inlet duty easily.

Apart from the positive results arising from such configuration in terms of process efficiency, a very important issue can be solved using this tool. The length of each OTM module is 25 cm, equal to its depth, while hundreds of chambers one on top of the other can bring about increasing heights: for instance a number of fluxes equal to 500 equals to a total height of the reactor of 4 meters. The ratio between the height and the base area of the single module would be too high, so connecting many reactors in series can increase the structural resistance of the equipment.

5.6 Parametric study conclusions and hints for an economic model

A synthesis of the previous analysis is given below (Table 11): one arrow stay for linear (or slow) growth while two arrows mean exponential growth.

Table 11: Parametric analysis synthesis

		Fuel conversion	Maximum Temperature	Net Heat	Inlet Duty
Number of stages	**Nstages**	↑	-	↑	-
Refrigeration Temperature	**Trefr**	↑	-	↑	-
Number of fluxes	**Nfluxes**	↑↑	↑↑	↑↑	-
Air Inlet Temperature	**TinOx**	↑↑	↑↑	↑↑	↑
Air Quantity Multiplicator	**a**	↑	↑	↑	↑
Number of parallel reactors	**U**	↑	↑	↑	-

One of the most important things that can be noticed is that, in general, *the system is controlled by oxygen permeation, being its rate the controlling step*[17]. For instance, equilibrium conversion is so high that an increase in temperature only favors substantially kinetics and mass transfer, or the effect of combustion in terms of heat generation prevails on the subsequent heating of air at the inlet of the reactors.

Moreover, the variables linked to the combustion reaction always grow *exponentially*, which leads to two reflections:

- CAPEX and OPEX tend to grow linearly, so the exponential shape of conversion and net heat production helps finding a working point of net profit for the plant.
- At the same time, a safety problem arises: the working point must ensure an efficient control of the system, to avoid runaway conditions – the overall net profit will be affected by this issue.

A *first guess* method to create an economical model is to decouple the variables. For instance, those which are not defined considering the multi-stage configuration, like the air inlet quantity and temperature, the number of membranes and the number of reactors in parallel can be used to calculate the overall inlet duties and to make sure that the maximum temperature is sufficiently low. Then, the number of stages can be related to conversion, while the

[17] In chemical reacting systems, the *rate determining step* it's the step taking place at the slowest rate, so that it defines the overall rate of the system.

refrigeration temperature (if it is lower than the inlet gas temperature[18]) can be regulated in order to obtain a net heat value higher than the overall inlet duty, without affecting the maximum temperature.

An example of such model is described below (Table 12). The values of molar flux and composition for 1 kg/h of PE undergoing pyrolysis at 400°C were used (Table 1: Weight yields for polyethylene pyrolysis [kg/kg of plastics],Table 4: Molar composition of the gas stream leaving the pyrolysis section for polyethylene[%]). Only one reactor is used ($u = 1$).

Table 12: Example of first guess combination of values for a gaseous stream coming from the pyrolysis of 1 kg/h of PE at 400 °C

Nstages	45	**Fuel conversion**	0.98
Nfluxes	400	**Maximum Temperature [°C]**	853.24
a	3	**Qtot [kJ/h]**	8.48e+5
TinOx [°C]	800	**Net Heat [kJ/h]**	1.07e+6
Trefr [°C]	400		

In the case of the objective pilot plant, an example configuration would be very different (Table 13: Example of first guess combination of values for a gaseous stream coming from the pyrolysis of 80 kg/h of PE at 400 °C):

Table 13: Example of first guess combination of values for a gaseous stream coming from the pyrolysis of 80 kg/h of PE at 400 °C

Nstages	60	**Fuel conversion**	0.94
Nfluxes	500	**Maximum Temperature [°C]**	871
a	3	**Qtot [kJ/h]**	7.03e+7
TinOx [°C]	800	**Net Heat [kJ/h]**	7.74e+7
Trefr [°C]	700		
u	20		

[18] If it is higher, it is not guaranteed that the maximum temperature at the outlet of the second step is lower than the one already considered.

Of course, this brings about some problems: for instance, it does not consider the growth of the CAPEX with the number of stages and the number of parallel reactors. The CAPEX can be so high that the economic balance of the plant as a whole can be affected, and even if a certain quantity of heat remains available for the rest of the plant, it does not overcome the investment fixed costs.

A solution to this problem is the generation of a single function of the considered variables, that accounts for all the costs in the plant, in first approximation: the *economic potential*.

6. Economic potential of the oxy-combustion plant section

6.1 Plant section configuration

The whole oxy-combustion plant section can be approximately represented by the following scheme (Figure 47: Simplified plant section scheme):

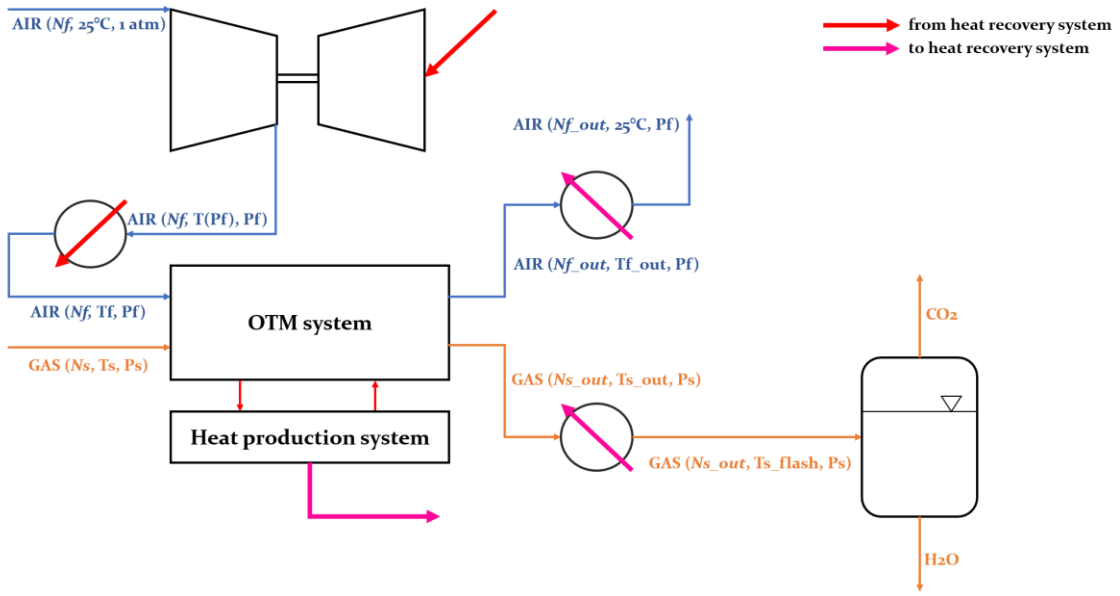

Figure 47: Simplified plant section scheme

It is composed by:

- The air compressor.
- The heat exchange facilities, a heater, for air at the inlet, and two coolers, for air and gas at the outlet.
- The OTM modules in series and the heat production system – made of a series of properly designed heat exchangers for gas cooling and air heating
- The flash vessel for water condensation.

The heat produced in the reactor is recycled inside the overall plant. First of all, a sufficient quantity is used to preheat the inlet gases to the reactor. Then, the needed quantity for the whole oxy-combustion operation must be subtracted by the overall heat balance (see 4.4). The remainder can be sent to the pyrolysis unit, in an outlook of efficient heat integration and energy saving – the main purpose of

this section of the plant. A scheme of heat integration in the whole plant is depicted below (Figure 48).

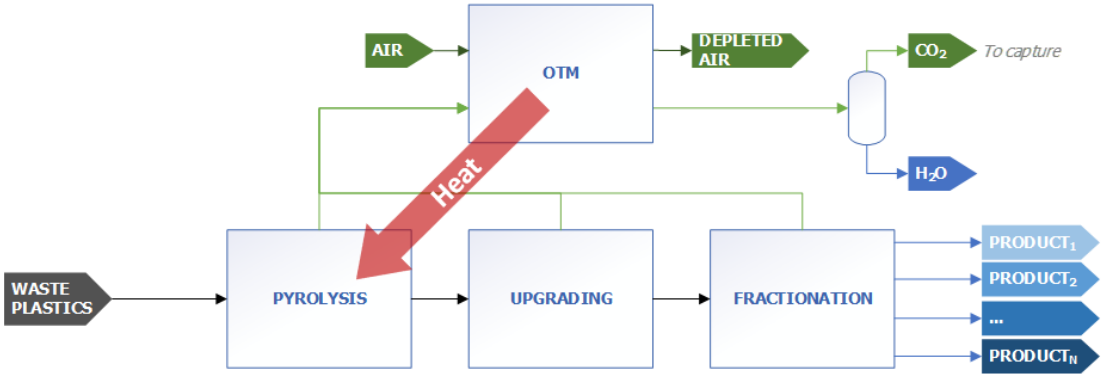

Figure 48: Heat integration scheme in the whole chemical recycle plant.

A certain quantity of energy is needed to operate the air compressor, and it is considered among the costs.

The stream containing carbon dioxide and water can be treated to separate them. Carbon dioxide can be captured and stored, for instance to be sold subsequently, while condensed water can be recycled inside the plant (if it is obtained from flashing with suitable purity); air, rich in nitrogen, can be discharged appropriately in the environment.

6.2 Economic potential calculation

The economic potential is a single value that accounts for all the revenues and cost related to a plant [66]. The idea is to create a function of the variables of interest, such as the independent variables discussed in section 5.2 and of the capacity of the plant. A suitable level of complexity is chosen for the calculations, depending on the needs of the analysis. In such context, due to the fact that the oxy-combustion section of the plant is just a *collateral*, necessary section, the function can be used to *minimize* overall costs in function of the quantity of heat produced in the plant section, its capacity, the chosen heat recovery configurations.

A possible equation for the calculation of the economic potential (*EP*) for the purpose is:

$$EP = €_{products} + €_{net\ heat} - €_{reactor} - €_{compr} - €_{h.e.} - €_{h.p.} \quad [€/h] \quad (40)$$

Where:

- $€_{products}$ = revenues from the products [€/h]. The only product is carbon dioxide, which has a value of around 25 €/t, so it is sufficient to multiply this value for the quantity of produced carbon dioxide.

  The cost of the reagents $€_{reagents}$ is considered null because, if there is[19], it is accounted for in the pyrolysis section.
- $€_{net\ heat}$ = economical value of the net heat obtained. So defined, it accounts for the generation of heat (for instance, in case of generation of *steam*) as heat that is not being bought to be used in the plant. If a convention is applied, for instance generation of steam at a certain pressure to be recycled in the plant, it is calculated as:

$$€_{net\ heat} = W_{steam} * €_{steam} = \frac{NetHeat * €_{steam}(P_{steam})}{\Delta H_{vap}^{steam}(P_{steam})} \quad [€/h] \quad (41)$$

  Where:

  - W_{steam} = quantity of steam produced by heating
  - P_{steam} = steam pressure
  - ΔH_{vap}^{steam} = enthalpy of vaporization of water in function of the steam pressure
  - $€_{steam}$ = economical value of the steam, in function of the steam pressure – for instance, 30 bar steam is worth 1.65 [€/1000 lb] while 70 bar steam 2.25 [€/1000 lb].

  Another convention that can be used for the revenues in terms of heat production could be its conversion to electric energy [67].
- $€_{reactor}$ = total cost of the reactor. The net value of the operation expenditure for the reactor is considered in the net heat revenues, so this term accounts only for the CAPEX.

[19] When it comes to plastic recycling, it is possible that not only raw material comes at no cost, but also that there are some economic benefits coming from government. At a higher level of complexity, transportation costs are to be taken into account.

This is composed by two terms:

$$€_{reactor} = €_{reactor}^{materials} + €_{reactor}^{production} \quad [€/h] \qquad (42)$$

The former, $€_{reactor}^{materials}$, refers strictly to the material of construction. It is a function of the number of modules and the number of membranes:

$$€_{reactor}^{materials} = \frac{€_{membrane} * N_{membranes} * N_{stages}}{t_{depreciacion}} \quad [€/h] \qquad (43)$$

Where:

- $€_{membrane}$ = cost of each membrane [€], given by the company KERIONICS – a single membrane has a cost of 86.71 €.
- $t_{depreciacion}$ = depreciation time, considered to amortize the installation costs. The plant has a lifetime of 20 years.

The second term, $€_{reactor}^{production}$, refers to the production costs of the membranes: the production method consists of cooking at 1400 °C for several hours, so the energy cost related with the process cannot be neglected.

At a higher level of complexity, these costs are made more precise with an addition: the indication of the cost of a necessary insulation system, not to lose heat in the environment.

- $€_{compr}$ = cost of the compression system. It is defined as:

$$€_{compr} = \frac{€_{compr}^{CAPEX}}{t_{depreciacion}} + €_{compr}^{OPEX} \quad [€/h] \qquad (44)$$

Where:

- $€_{compr}^{CAPEX}$ = equipment installation cost [€], calculated with Guthrie's formula [66]:

$$€_{compr}^{CAPEX} = 517.5 * \frac{M\&S}{280} * (bhp)^{0.82} * (2.11 + F_c) \quad [€] \qquad (45)$$

Where:

- *M&S* = Marshall & Swift index. It is based on an average of costs, and accounts for the *yearly inflation* with respect to a given year at which the price of a certain equipment is known. In fact, 280 is the M&S index of 1969, so the ratio between the two values gives a multiplicator of costs for the current year.
- *bhp* = brake horsepower, which is the power of the compressor *Qcomp* expressed in *hp* divided by the *efficiency* of the compressor.
- F_c is a constant that depends on the type of compressor. It is equal to 1 for a *centrifugal compressor* – a reciprocating compressor is not suggested due to the high flow rates and the low pressure differences.

- $€_{compr}^{OPEX}$ = operative expenditure of the compressor, intended as the cost of the high pressure steam required to give the compressor the required energy to work:

$$€_{compr}^{OPEX} = Q_{comp} * €_{electr} \quad [€/h] \qquad (46)$$

Where $€_{electro}$ is the cost of electricity, in the country of interest [67]. It is more accurate to calculate the cost in terms of electrical energy due to the very functioning of the gas compressor.

Usually, costs related to compression are among the highest. In this case, they shall not be very high, due to the low relevance that a high pressure has on the overall outcome of the reaction, as discussed (see 5.3). Such result lead to a high advantage in terms of costs reduction, both in CAPEX and OPEX.

- $€_{h.e.}$ = cost of the heat exchange system, It includes three terms: one related to the air heater at the reactor inlet, one related to the gas cooler at the flash inlet, one related to the equipment to the air cooler before discharge. Each of the three terms is the sum of:
  - A CAPEX term, depreciated over 20 years as seen in the previous cases [66]:

$$€_{h.e.}^{CAPEX} = 101.3 * \frac{M\&S}{280} * A^{0.65} * (2.29 + F_{he}) \quad [€] \qquad (47)$$

Where:

- A = exchange area, calculated as:

$$A = \frac{Q_{exch}}{U_h * LMTD} \quad [m^2] \qquad (48)$$

Where:

- Q_{exch} = the exchanged heat [W]
- U_h = global heat transfer coefficient [W/m^2/K]. It depends on the type of heat exchanger (Kettle reboiler, condenser etc.), on the type of utility, on the range of temperature[20].
- *LMTD* = logarithmic mean temperature difference across the heat exchanger[21].

- F_{he} = a constant accounting for the heat exchanger typology, the building material, and the working pressure [66].

- An OPEX term, defined as above, and considered positive if it is an expense, due to the shape of the equation:
  - For the air heater, it is positive and defined in terms of steam consumption cost.
  - For the gas and air coolers, it is negative and defined as the steam production revenues, as for the term related to the net heat.

- $€_{h.p.}$ = cost of the heat production section. The OPEX term is already considered in the net heat production term, so these terms should account for the CAPEX only.

[20] Usually, average values for the global transfer coefficient can be used in function of the equipment – for instance for a condenser it is around 580 W/m^2/K.

[21] Being A and B the sides of a heat exchanger and ΔT the temperature difference across the two exchanging fluids, *LMTD = (ΔTA – ΔTB)/(ln(ΔTA/ΔTB))*F* where *F* is a correction factor accounting for the path followed by tubes – for instance, single passage countercurrent or double passage.

This is calculated following the guidelines given above (eq. (47) and (48)): the heat exchange area combined with information like the type of material and the working pressure, give information about the quantity of material to be bought and its cost. It is also a function of the number of OTM stages in series. This topic is treated in section 7.2.2.

By observing the shape of the function and of the terms that compose it, it can immediately be seen that:

- For a given molar flow of gases and a given fuel conversion, the revenue from the products is fixed. The revenue that can increase is given by the combination of variables that allow the highest net production of heat, by decreasing the air heat need.
- As previously mentioned, the CAPEX part of the equation is affected by the reactor and the heat exchange system, because the compressor investment costs are reduced due to the low effects that pressure has on the system.
- OPEX is affected by the overall electric and thermal energy required.

As a consequence, to these considerations, various configurations can be compared, and the optimal configuration can be found by calculating the *maximum economic potential*. This can be achieved by implementing a function for such economic potential calculation in MATLAB®, to automatically obtain the corresponding values in function of the input variables.

However, the equation is elaborated at a certain level of approximation, so there are more expenses to be considered – such as maintenance costs, manpower costs, costs for compression and storage of the outlet carbon dioxide, and so on. It is a suitable starting point for a more detailed design of the plant section.

7. Conclusions and further developments

This chapter synthetizes the conclusions reached in the study and resumes the hints for further developments of the technology in its entirety, for a final design and start up for the chemical recycle plant.

7.1 Conclusions of the thesis

Using the method explained above (Figure 12) it was possible to:

- **Create a theoretical model**, which correctly describes the evolution of the variables of interest in the system. Such operation allowed a better comprehension of the evolution of the system, under suitable hypotheses and in the operative conditions considered, and the bases for a numerical implementation of it – using any software, being not necessarily MATLAB®.
- **Implement the model in MATLAB®**. This operation allowed anyone to perform simulations of a hypothetical system, having *any* mass fluxes, composition, temperatures, pressures, structural dimensions of the reactor. Also, it was possible to see that a multi-stage configuration was needed for an efficient exploitation of temperature rises of the gases, and to model it.
  Use the numerical solution obtained in MATLAB®, coupled with data from ASPEN HYSYS®, to **perform a parametric study** of the OTM membrane reactor system. It was very useful to obtain an overview of the effects of the main input variables on the system: some variations were not trivial (see for instance Figure 36) and the overall analysis allowed to seek a combination of variables to obtain the desired output result.
- **Elaborate an overall economic potential model**, which could give information about the optimal reactor configuration in function of all the variables. It could allow a better comprehension of the overall economy of the plant, in a qualitative way, and also give the bases for a more accurate numerical implementation, in the decision-making step of the plant design process.

This whole study was very useful to have a better understanding of the evolution of the reacting system and of the measures required to control temperature and conversion, and to obtain first guess values of produced combustion heat at high conversions, heat requirements for the process, and temperatures involved in the process.

7.2 Further developments

Possible further developments of the whole project can be achieved in the long term, in mainly three fields: the structure of the reacting system, in terms of materials and configuration of the membrane module; the design of the heat recovery system; the numerical simulation of the oxy-combustion plant section.

7.2.1 Improvement of the OTM structure

The OTM system undergoes continuous analysis for its improvement [50]: the choice of different materials and their structure inside the membrane is object of study because of its possible incredible effects on the overall economy of the plant.

An increase of the oxygen flux across the membrane, at equal exchange area, causes a linear increase of conversion if the plant configuration and conditions are left unchanged (Figure 49**Errore. L'origine riferimento non è stata trovata.**): b is a factor, greater than one, that multiplies the oxygen flux J_{O_2} as it is currently defined, at each step of the integration.

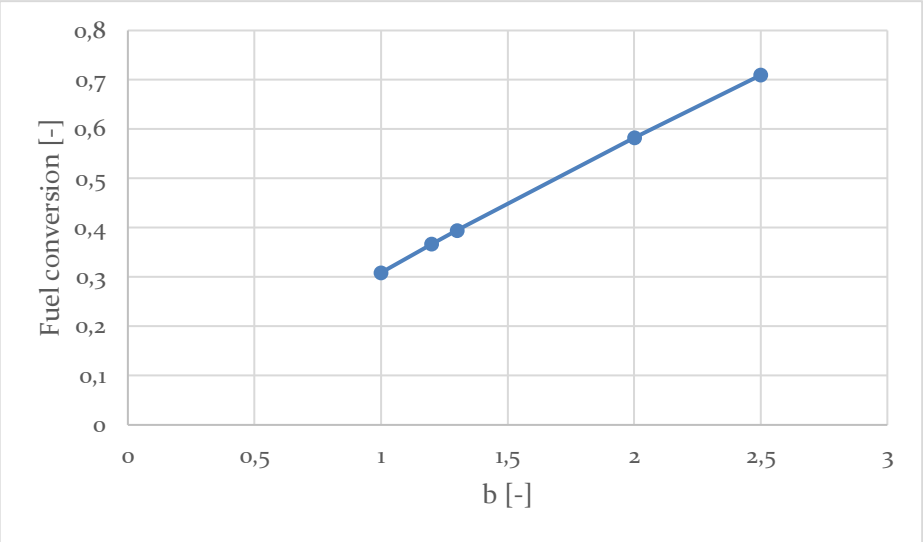

Figure 49: Dependence of fuel conversion on the oxygen flux multiplication factor. JO2_real = b·JO2

Such a result could be achieved by developing new materials (or mix of materials, see 1.5) which allow higher oxygen rates, or membrane configurations where the dense thickness of the membrane is lower (Figure 14)

It is sufficient to double the flux of oxygen, to double the fuel conversion. This means that, at equal conversion, the number of stages (Figure 24) and the number of fluxes (Figure 26) can decrease in a linear fashion. A similar improvement can have positive consequences in the plant in terms of CAPEX, but also in terms of saved space for the reactor.

Another important improvement in the selection of materials of the membrane, but also of the overall structure, could be in terms of *thermal resistance*. As seen before, there is a correspondence between higher fuel conversions and higher temperatures reached in the modules of the reactor. If future developments allowed increasing the maximum temperature accepted in the reactor, then the reaction could take place in more extreme conditions, and investment costs (number of stages, number of heat exchange devices) would be reduced.

Also, the overall structure of a single module can be changed. The theoretical transport model takes the length of the chamber as characteristic dimension of the heat transfer due to the very low height of the chamber with respect to the length, but if the height of the chamber is increased, changes take place in terms of output

results. As the height of the chamber increases, keeping the total inlet area (or equally the inlet height, see equation (4)) constant by changing the number of membranes in the module, the fuel conversion decreases (Figure 50):

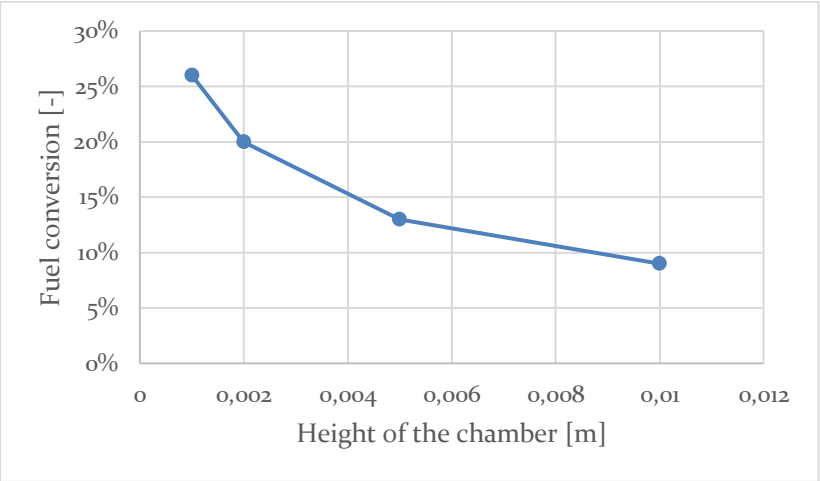

Figure 50: Dependence of the fuel conversion on the height of the single chamber, keeping the total height of the OTM module constant

This is due to the fact that, if seen the other way around, at equal height of the overall reactor, there are less membranes. The area of exchange for oxygen permeation lowers, and so does the fuel conversion. Also, increasing the height of the chamber also leads to lower heat transfer coefficient across the chambers, by increasing the actual distance between them.

The optimum height of the chamber can be found, in function of the desired conversion, on whose value depends the profit from carbon dioxide production and heat generation, and expenses for the production of the membranes and stages. A lower height can bring advantages in terms of saved space, too.

7.2.2 Design of the heat production system

As seen above (sections 4.4 and 6.2), a heat production system is needed to exploit the energy released by combustion at its best and to maintain safe conditions in the various stages of the reactor. There can be various alternatives to its design, which can vary in terms of construction, heat production method, and costs. The choice of the heat production system can have great outcomes in the overall plant section economic potential, besides affecting the space occupied by the equipment and the safety and control of the system.

The easiest, most intuitive system could be a series of heat exchangers, for instance in the form of reboilers and condensers, to produce or consume steam for the considered purposes. However, due to the fact that the heat production section is very complex, the choice of several heat exchangers in series may not be the most sensible choice, in terms of space saving and of complexity of the control system. If the number of stages is too high, a non-conventional unit can be designed for the task, for instance to save some space and some building material, or to have a better engineered connection of the produced steam, between the heat generation side and the heat need side. For instance, an integrated system of heat recovery can also be taken into account: a single piece of equipment built as a huge boiler in which all the streams concur to the formation of steam. This has the advantage of buying, handling and possibly maintaining a single instrument, but intuitively the control in required temperatures for each stage of the reactor is lower. Also, another piece of equipment should be integrated to supply the air heating need at each step of the reactor. Nevertheless, it must also be considered that the design of a non-conventional, specific unit could result in a very high expense.

It could also be interesting to design a *direct heating* system: hot gases leaving each step of the OTM reactor could be refrigerated in contact with other units inside the plant which require heat. Such units could be the pyrolysis reactor, or an upstream unit to melt plastic before entering the pyrolysis section, or even subsequent, catalytic steps. Such a solution should allow an efficient heat integration inside the plant, avoiding heat losses which are inevitable when real equipment efficiencies are considered. and a reduction in investment costs of indirect production of heat.

7.2.3 Integrated simulation and control of the plant section

The numerical simulation presented in this work is enough for *first guess* considerations on the dimensions of the reactor and on heat production and consumptions directly connected to the oxy-combustion system. For a more precise design and sizing of all the pieces of equipment in the plant and a more detailed integration of the heat duties and resources, MATLAB® itself cannot supply sufficient tools for the task. Nevertheless, the simulation of a non-

conventional unit such as a membrane reactor is easier and more precise using MATLAB®, so this numerical algorithm is necessary in this phase of the project.

A further step leading to the final objective of the companies, comprehending design, simulation, and integrated control of the oxy-combustion section in a pilot plant, would be the connection of the MATLAB® numerical solution to a more detailed plant sheet in ASPEN HYSYS® or in the ASPEN PLUS® suite, or to a dynamic control suite like AVEVA© DYNSIM dynamic simulator.

Such an integrated system between two (or more) informatic tools should allow:

- Real time calculation of produced heat and heat duties
- Sizing of equipment and easy calculation of its cost, such as heat exchangers, compressors, turbines etc.
- Simulation of start-up and shut-down conditions, instead of just the steady state simulation
- Iterative optimization of variables

This requires the connection between one environment and the other, to exchange information. A possible scheme for a plant simulation environment like ASPEN HYSYS® is provided below (Figure 51**Errore. L'origine riferimento non è stata trovata.**):

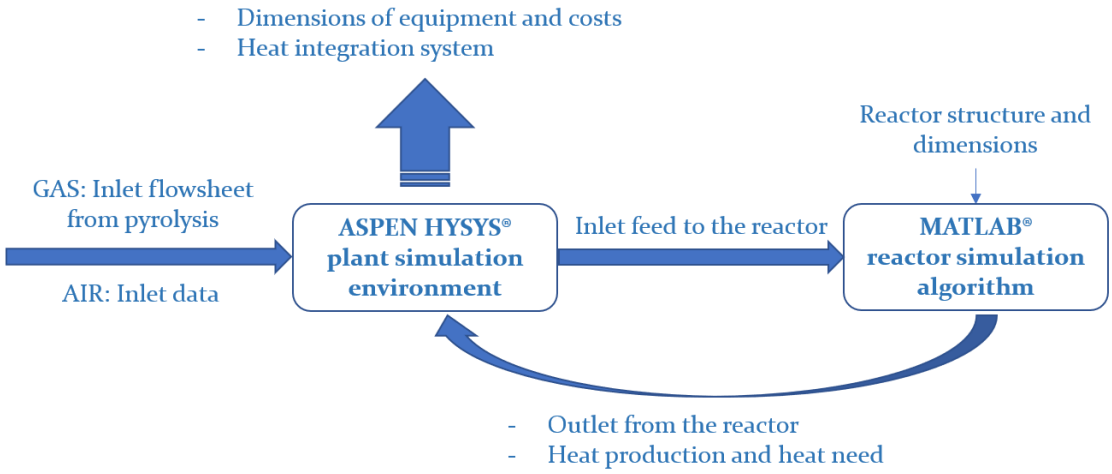

Figure 51: Integrated plant simulation example, with a connection between MATLAB® and ASPEN HYSYS® environments

Bibliography

[1] PlasticsEurope, "Plastics - The Facts 2019," 2019.

[2] PlasticsEurope, "Plastics - The Facts 2015," 2015.

[3] PlasticsEurope, "Plastics - The Facts 2016," 2016.

[4] PlasticsEurope, "Plastics - The Facts 2017," 2017.

[5] PlasticsEurope, "Plastics - The Facts 2018," 2018.

[6] PlasticsEurope, "The Circular Economy for Plastics – A European Overview".

[7] N. Singh, D. Hui, R. Singh, I. Ahuja, L. Feo and F. Fraternali, "Recycling of plastic solid waste: A state of art review and future applications," no. Composites Part B 115 (2017) 409-422.

[8] iCAREPLAST, [Online]. Available: https://www.icareplast.eu/project-details/.

[9] E. Commission, "COMMISSION REGULATION (EC) No 2023/2006 of 22 December 2006 on good manufacturing practice for materials and articles intended to come into contact with food," 2006.

[10] A. Veksha, A. Giannis, W.-D. Oh, V. Chang and G. Lisak, "., Upgrading of non-condensable pyrolysis gas from mixed plastics through catalytic decomposition and dechlorination," Vols. Fuel Processing Technology, 2018. 170: p. 13-20..

[11] J. Park, K. Park, J.-S. Kim, S. Maken, H. Song, H. Shin and e. al., "Characterization of Styrene Recovery from the Pyrolysis of Waste Expandable Polystyrene," Vols. Energy & Fuels, 2003. 17(6): p. 1576-1582.

[12] S.-H. Jung, M.-H. Cho, B.-S. Kang and J.-S. Kim, "Pyrolysis of a fraction of waste polypropylene and polyethylene for the recovery of BTX aromatics using a fluidized bed reactor," Vols. Fuel Processing Technology, 2010. 91(3): p. 277-284.

[13] A. Aboulkas, T. Makayssi, L. Bilali, K. El harfi, M. Nadifiyine and M. Benchanaa, "Co-pyrolysis of oil shale and plastics: Influence of pyrolysis parameters on the product yields," Vols. Fuel Processing Technology, 2012. 96: p. 209-213.

[14] I. Ahmad, M. Khan, H. Khan, M. Ishaq, R. Tariq, K. Gul and e. al., "Pyrolysis Study of Polypropylene and Polyethylene Into Premium Oil Products," Vols. International Journal of Green Energy, 2015. 12(7): p. 663-671..

[15] J. Mark, Physical properties of polymers handbook. Vol 1076., Springer, 2007.

[16] P. P. Database, "Heat Capacity of Liquid and Solid Polymers at 298 K," 2015. [Online]. Available: http://polymerdatabase.com/polymer%20physics/Cp%20Table2.html.

[17] P. P. Database, "Heat Capacity of Polymers," 2015. [Online]. Available: https://polymerdatabase.com/polymer%20physics/HeatCapacity.html.

[18] R. Blaine, "Polymer heats of fusion. TA Instruments, New Castle, DE.," 2002. [Online]. Available: www. tainstruments. com/library_download.aspx.

[19] K. Tanoue, M. Nagao, A. Yoshida and T. Nishimura, "Heat transfer and phase change in a polystyrene packed bed during melting," Vols. International Journal of Heat and Mass Transfer, 2014. 79: p. 324-331.

[20] R. Bagri and W. P.T., "Catalytic pyrolysis of polyethylene," Vols. Journal of Analytical and Applied Pyrolysis, 2002. 63(1): p. 29-41.

[21] K. Murata, K. Sato and Y. Sakata, " Effect of pressure on thermal degradation of polyethylene," Vols. Journal of Analytical and Applied Pyrolysis, 2004. 71(2): p. 569-589..

[22] J. Onwudili, N. Insura and P. Williams, "Composition of products from the pyrolysis of polyethylene and polystyrene in a closed batch reactor: Effects of temperature and residence time," Vols. Journal of Analytical and Applied Pyrolysis, 2009. 86(2): p. 293-303.

[23] M. Seifali Abbas-Abadi, M. Nekoomanesh Haghighi, A. McDonald and Y. H., "Estimation of pyrolysis product of LDPE degradation using different process parameters in a stirred reactor," Vols. Polyolefins Journal, 2015. 2(1): p. 39-47.

[24] M. Seifali Abbas-Abadi, M. Haghighi, H. Yeganeh and A. McDonald, "Evaluation of pyrolysis process parameters on polypropylene degradation products," vol. J Anal Appl Pyrolysis 2014;109:272–7..

[25] G. Elordi, G. Lopez, M. Olazar, R. Aguado and J. Bilbao, "Product distribution modelling in the thermal pyrolysis of high density polyethylene," Vols. Journal of Hazardous Materials, 2007. 144(3): p. 708-714.

[26] G. Sulistyo, "Kinetics Modeling of Waste Plastic Mixture Pyrolysis for Liquid Fuel Production," Vols. International Journal of Innovative Technology and Exploring Engineering, 2019. 8(5)..

[27] A. Demirbas, " Pyrolysis of municipal plastic wastes for recovery of gasoline-range hydrocarbons," Vols. Journal of Analytical and Applied Pyrolysis, 2004. 72(1): p. 97-102..

[28] J. Mertinkat, A. Kirsten, M. Predel and W. Kaminsky, "Cracking catalysts used as fluidized bed material in the Hamburg pyrolysis process," Vols. Journal of Analytical and Applied Pyrolysis, 1999. 49(1): p. 87-95..

[29] Y. Kim, G. Hwang, S. Bae, S. Yi, S. Moon and H. Kumazawa, "Pyrolysis of polystyrene in a batch-type stirred vessel," Vols. Korean Journal of Chemical Engineering, 1999. 16(2): p. 161-165.

[30] S. Imani Moqadam, M. Mirdrikvand, B. Roozbehani, A. Kharaghani and M. Shishehsaz, "Polystyrene pyrolysis using silica-alumina catalyst in fluidized bed reactor," Vols. Clean Technologies and Environmental Policy, 2015. 17(7): p. 1847-1860.

[31] M. Rezvanipour, H. Alikhani and M. Pazouki, "Catalytic pyrolysis of general purpose polystyrene using red mud as a catalyst," Vols. Iranian Journal of Chemical Engineering Vol. 11, No. 4 (Autumn 2014).

[32] Z. Tamri, A. Vaziri Yazdi, M. Nekoomanesh Haghighi and H. A. Seifali Abbas-Abadi M., "Effect of temperature, heating rate and zeolite-based catalysts on the pyrolysis of high impact polystyrene (HIPS) waste to produce fuel-like products," Vols. Polyolefins Journal, 2019. 6(1): p. 43-52.

[33] S. Krishna Kant Kumar Singh, "Kinetic Model Analysis for Pyrolysis of Waste Polystyrene Over Laumontite," Vols. International Journal of Engineering Research & Technology, 2013. 2(2).

[34] A. Karaduman, E. Şimşek, B. Çiçek and A. Bilgesü, "Thermal degradation of polystyrene wastes in various solvents," Vols. Journal of Analytical and Applied Pyrolysis, 2002. 62(2): p. 273-280.

[35] V. Chumbhale, J.-S. Kim, S.-B. Lee and M.-J. Choi, "Catalytic degradation of expandable polystyrene waste (EPSW) over mordenite and modified mordenites," vol. J Mol Catal A Chem 2004;222:133–41.

[36] E. Stocchi, Chimica Industriale - Organica vol. 2, Edisco, 1990.

[37] S. Smart, C. X. C. Lin, L. Ding, K. Thambimuthu and J. C. Diniz da Costa, "Ceramic Membranes for Gas Processing in Coal Gasification," Vols. Energy Environ. Sci. 2010, 3, 268-278.

[38] K. Brooks, "Perovskite," no. Geology Today 36(1) (2020) 33-38.

[39] A. F. Holleman and E. Wiberg, Inorganic Chemistry, Academic Press/De Gruyter, 2001.

[40] C. Chen, B. Boukamp, H. Bouwmeester, G. Cao, H. W. A. Kruidhof and A. Burggraaf, "Microstructural development, electrical properties and oxygen permeation of zirconia-palladium composites," Vols. Solid State Ionics, 76 (1995) 23-28.

[41] C. Chen, H. Kruidhof, H. Bouwmeester, H. Verweij and A. Burggraaf, "Oxygen permeation through oxygen ion oxide-noble metal dual phase composites," Vols. Solid State Ionics, 86-88, Part 1 (1996) 569-572.

[42] J. Kim and Y. Lin, "Synthesis and oxygen permeation properties of ceramic-metal dual-phase membranes," Vols. J. Membr. Sci., 167 (2000) 123-133.

[43] H. Luo, H. Jiang, K. Efimov, F. Liang, H. Wang and J. Caro, "CO2-Tolerant Oxygen-Permeable Fe2O3-Ce0.9Gd0.1O2-δ Dual Phase Membranes," Vols. Industrial & Engineering Chemistry Research, 50 (2011) 13508-13517.

[44] H. Luo, H. Jiang, T. Klande, Z. Cao, F. Liang, H. Wang and J. Caro, "Novel Cobalt-Free, Nobel Metal-Free Oxygen-Permeable 40Pr(0.6)Sr(0.4)FeO(3-δ)-60Ce(0.9)Pr(0.1)O(2-δ), Dual-Phase Membrane," Vols. Chemistry of Materials, 24 (2012) 2148-2154.

[45] J. Garcia Fayos, M. Balaguer and J. M. Serra, "Dual-Phase Oxygen Transport Membranes for Stable Operation in Environments Containing Carbon Dioxide and Sulfur Dioxide," Vols. ChemSusChem. 2015 Dec 21;8(24):4242-9.

[46] J. Kniep, Q. Yin, I. Kumakiri and Y. Lin, "Electrical conductivity and oxygen permeation properties of SrCoFeOx membranes," Vols. Solid State Ionics, 180 (2010) 1633-1639.

[47] K. Yun, C.-Y. Yoo, S.-G. Yoon, J. H. Yu and J. H. Joo, "Chemically and thermo-mechanically stable LSM-YSZ segmented oxygen permeable ceramic membrane," Vols. Journal of Membrane Science, 486 (2015) 222-228.

[48] C. Rizescu and M. Rizescu, Structure of Crystalline Solids, Imperfections and Defects in Crystals, Parker, TX: Shutter Waves, 2018.

[49] Y.-S. Ling, W. Wang and J. Han, "Oxygen Permeation through Thin Mixed-Conducting Solid Oxide Membranes," no. AIChE J. 40 (5) (1994) 786.

[50] J. García Fayos, Universitat Politècnica de València, 2017.

[51] A. L. E. E. Kayode Coker, "Appendix C: Physical Properties of Liquids and Gases," in *Ludwig's Applied Process Design for Chemical and Petrochemical Plants: Distillation, packed towers, petroleum fractionation, gas processing and dehydration*, Elsevier Science & Technology, 2019.

[52] R. H. Perry and D. W. Green, Perry's Chemical Engineers' Handbook, McGraw-Hill, 2007.

[53] C. Li, J. J. Chew, A. Mahmoud, S. Liu and J. Sunarso, "Modelling of oxygen transport through mixed ionic-electronic conducting (MIEC) ceramic-based membranes: An overview," no. Journal of Membrane Science 567 (2018) 228–260.

[54] S. J. Xu and W. J. Thompson, "Oxygen permeation rates through ion-conducting perovskite," no. Chemical Engineering Science 54 (1999) 3839-3850.

[55] J. Hong, P. Kirchen and A. F. Ghoneim, "Numerical simulation of ion transport membrane reactors: Oxygen permeation and transport and fuel conversion," no. Journal of Membrane Science 407– 408 (2012) 71– 85.

[56] "Fuel Gases Heating Values," 2005. [Online]. Available: https://www.engineeringtoolbox.com/heating-values-fuel-gases-d_823.html.

[57] C. K. Westbrook and F. L. Dryer, "Simplified Reaction Mechanisms for the Oxidation of Hydrocarbon Fuels in Flames," no. Combustion Science and Technology 27(1-2) 31-43.

[58] C. Yin, "Advanced modeling of oxy-fuel combustion of natural gas".

[59] T. L. Bergman, Fundamentals of heat and mass transfer, John Wiley & Sons, 2011.

[60] "CHECALC," [Online]. Available: https://checalc.com/solved/multi_flash.html.

[61] C. Wilke, "A Viscosity Equation for Gas Mixtures," no. The Journal of Chemical Physics 18 (1950) 517–519.

[62] L. F. Shampine, I. Gladwell and S. Thompson, Solving ODEs with Matlab, Cambridge University press, 2003.

[63] J. C. Butcher, Numerical Methods for Ordinary Differential Equations, John Wiley & Sons, 2016.

[64] A. Cuoci, A. Frassoldati, T. Faravelli and E. Ranzi, "OpenSMOKE++: An object-oriented framework for the numerical modeling of reactive systems with detailed kinetic mechanisms," no. Computer Physics Communications 192 (2015) 237–264.

[65] H. Topsoe, "Topsoe.com," [Online]. Available: https://www.topsoe.com/processes/ammonia.

[66] J. M. Douglas, Conceptual Design of Chemical Processes, McGraw Hill Book Company, 1988.

[67] GlobalPetrolPrices, "Electricity prices," [Online]. Available: https://www.globalpetrolprices.com/electricity_prices/.

[68] J. H. Joo, K. S. Yun, Y. Lee, J. Jun, C.-Y. Yoo and J. H. Yu, "Dramatically Enhanced Oxygen Fluxes in Fluorite-Rich Dual-Phase Membrane by Surface Modification," no. Chemistry of Materials 26 (2014) 4387-4394.

[69] H. Bouwmeester, H. Kruidhof and A. Burgggraaf, "Importance of the surface exchange kinetics as rate limiting step in oxygen permeation through mixed-conducting oxides," no. Solid State Ionics 72 (1994) 185-194 .

[70] S. Arrhenius, "Über die Dissociationswärme und den Einfluß der Temperatur auf den Dissociationsgrad der Elektrolyte," no. Z. Phys. Chem. 4 (1889) 96–116.

[71] IEN, "Deliverable 5.2 CFD Simulation of syngas/natural gas co-combustion," 2018.

Appendix A

```
%% Effective concentration^lambda [(mol/m3)^lambda]
% C = concentration
% lambda = order of reaction of component C in the reaction
function C_pow_lambda = Ceff(C, lambda)

if lambda == 0.
    C_pow_lambda=1;
else
    if (lambda>=1.)
        C_pow_lambda = C^lambda;
    else
        Cstar = 1.e-40;
        ALFA = 1.e-3;
        H = 1.50*log(ALFA / (1. - ALFA));
        K = 2.00*log((1. - ALFA) / ALFA) / Cstar;
        delta = 1.e9;
        m = (tanh(K*C + H) + 1.) / 2.;
        gamma = m*(C + m / delta)^lambda + (1. -
m)*Cstar^(lambda - 1.)*C;

        C_pow_lambda = gamma;
    end
end
end
```

Appendix B

```
%% ODE solution
Nstages = 45;
h_step = 0.00001;
xspan = [0 Ltot];
options = odeset('MaxStep', h_step);

solution = ode15s(@ODE_OTM, xspan, [Ns_in Tin NfO2_in
TinOx], options);

x_end = solution.x;
Ns_end = solution.y(1:Ncomp,:);
Ts_end = solution.y(Ncomp+1,:)-273.15;
Nf_O2_end = solution.y(Ncomp+2,:);
Tf_end = solution.y(Ncomp+3, :)-273.15;

% Cooling stages calculations

Tin = 400 + 273.15;

intcpvw = integral(@SpecificHeatWater, 25+273.15, Tv);
%J/mol
Fgas = sum(Ns_end(:, end));      %mol/s
xgas = Ns_end(:, end)/Fgas;      %-
intcpvgas = IntegralCpvGas(xgas, Tin, Ts_end(end)+273.15);
%J/mol
HeatGeneration = zeros(1, Nstages);
HeatGeneration(1) = Fgas*intcpvgas;      %J/s


%Air Heating Stages
Fair = (Nf_O2_end(end) + nN2);
xair = [Nf_O2_end(end) nN2]/Fair;
intcpvair = IntegralCpvAir(xair, Tf_end(end)+273.15,
TinOx);
HeatNeed = zeros(1, Nstages);
HeatNeed(1) = Fair*intcpvair;

%Inlet sweep and feed composition
Ns_in = Ns(:, end)';
NfO2_in = Nf_O2(end);

%T = T inlet to the reactor, F = total molar flux of gas, x
= composition
%of gas, T2 = T outlet from the reactor

for t = 2:Nstages

xspan = [Ltot*(t-1) Ltot*t];
```

```
solution = ode15s(@ODE_OTM, xspan, [Ns_in Tin NfO2_in
TinOx], options);
x1 = solution.x;
Ns = solution.y(1:Ncomp,:);
Ts_sol = solution.y(Ncomp+1,:)-273.15;
Nf_O2 = solution.y(Ncomp+2,:);
Tf_sol = solution.y(Ncomp+3, :)-273.15;

Ns_end = horzcat(Ns_end, Ns);
Ts_end = horzcat(Ts_end, Ts_sol);
Tf_end = horzcat(Tf_end, Tf_sol);
Nf_O2_end = horzcat(Nf_O2_end, Nf_O2);
x_end = horzcat(x_end, x1);

Ns_in = Ns_end(:, end)';
NfO2_in = Nf_O2_end(end);

%Heat Generation calculations
Fgas = sum(Ns_end(:, end));
xgas = Ns_in/Fgas;
intcpvgas = IntegralCpvGas(xgas, Tin, Ts_end(end)+273.15);
HeatGeneration(t) = Fgas*intcpvgas;

%Heat Need calculations
Fair = (Nf_O2_end(end) + nN2);
xair = [Nf_O2_end(end) nN2]/Fair;
intcpvair = IntegralCpvAir(xair, Tf_end(end)+273.15,
TinOx);
HeatNeed(t) = Fair*intcpvair;
end

%% Some outlet data
conversion = Ns_end(2, end)/(Ns_in_tot_v(5)/N_flux);
Ngasouttot = Fgas*N_flux;
Nairouttot = (Nf_O2_end(end) + nN2)*N_flux;
HeatGenTot = sum(HeatGeneration)*N_flux*10^-3*60*60; %kJ/h
HeatNeedTot = sum(HeatNeed)*N_flux*10^-3*60*60; %kJ/h

function integral = IntegralCpvGas(x, T1, T2)
%cpv = cpv_a + cpv_b*T + cpv_c*T^2 + cpv_d*T^3 + cpv_e*T^4
[J/mol/K], T in K
%[O2 CO2 H2 H2O CH4]
cpv_a = [29.526 27.437 25.399 33.933 34.942];
cpv_b = [-8.8999e-3 4.2315e-2 2.0178e-2 -8.4186e-3 -
3.9957e-2];
cpv_c = [3.8083e-5 -1.9555e-5 -3.8549e-5 2.9906e-5 1.9184e-
4];
cpv_d = [-3.2629e-8 3.9968e-9 3.1880e-8 -1.7825e-8 -
1.5303e-7];
cpv_e = [8.8607e-12 -2.8972e-13 -8.7585e-12 3.6943e-12
3.9321e-11];
```

```
int = cpv_a*(T2-T1) + cpv_b/2*(T2^2-T1^2) + cpv_c/3*(T2^3-
T1^3) + cpv_d/4*(T2^4-T1^4) +cpv_e/5*(T2^5-T1^5);

integral = dot (x, int);
end

function integral = IntegralCpvAir(x, T1, T2)
%cpv = cpv_a + cpv_b*T + cpv_c*T^2 + cpv_d*T^3 + cpv_e*T^4
[J/mol/K], T in K
%[O2 N2]
    cpv_a = [29.526 29.342];
    cpv_b = [-8.8999e-3 -3.5395e-3];
    cpv_c = [3.8083e-5 1.0076e-5];
    cpv_d = [-3.2629e-8 -4.3166e-9];
    cpv_e = [8.8607e-12 2.5935e-13];

int = cpv_a*(T2-T1) + cpv_b/2*(T2^2-T1^2) + cpv_c/3*(T2^3-
T1^3) + cpv_d/4*(T2^4-T1^4) +cpv_e/5*(T2^5-T1^5);

integral = dot (x, int);
end
```